

## Discovery of Potent and Selective Inhibitors of Cdc2-like Kinase 1 (CLK1) as a New Class of Autophagy Inducers

Qi-Zheng Sun, Gui-Feng Lin, Lin-Li Li, Xi-Ting Jin, Lu-Yi Huang, Guo Zhang, Wei Yang, Kai Chen, Rong Xiang, Chong Chen, Yu-Quan Wei, Guang-Wen Lu, and Sheng-Yong Yang

*J. Med. Chem.*, **Just Accepted Manuscript** • DOI: 10.1021/acs.jmedchem.7b00665 • Publication Date (Web): 10 Jul 2017

Downloaded from <http://pubs.acs.org> on July 10, 2017

### Just Accepted

“Just Accepted” manuscripts have been peer-reviewed and accepted for publication. They are posted online prior to technical editing, formatting for publication and author proofing. The American Chemical Society provides “Just Accepted” as a free service to the research community to expedite the dissemination of scientific material as soon as possible after acceptance. “Just Accepted” manuscripts appear in full in PDF format accompanied by an HTML abstract. “Just Accepted” manuscripts have been fully peer reviewed, but should not be considered the official version of record. They are accessible to all readers and citable by the Digital Object Identifier (DOI®). “Just Accepted” is an optional service offered to authors. Therefore, the “Just Accepted” Web site may not include all articles that will be published in the journal. After a manuscript is technically edited and formatted, it will be removed from the “Just Accepted” Web site and published as an ASAP article. Note that technical editing may introduce minor changes to the manuscript text and/or graphics which could affect content, and all legal disclaimers and ethical guidelines that apply to the journal pertain. ACS cannot be held responsible for errors or consequences arising from the use of information contained in these “Just Accepted” manuscripts.

1  
2  
3  
4  
5  
6  
7  
8  
9  
10  
11  
12  
13  
14  
15  
16  
17  
18  
19  
20  
21  
22  
23  
24  
25  
26  
27  
28  
29  
30  
31  
32  
33  
34  
35  
36  
37  
38  
39  
40  
41  
42  
43  
44  
45  
46  
47  
48  
49  
50  
51  
52  
53  
54  
55  
56  
57  
58  
59  
60

1  
2  
3  
4 **Discovery of Potent and Selective Inhibitors of Cdc2-like Kinase 1 (CLK1) as a**  
5  
6 **New Class of Autophagy Inducers**  
7

8 Qi-Zheng Sun,<sup>†,§</sup> Gui-Feng Lin,<sup>†,§</sup> Lin-Li Li,<sup>‡,§</sup> Xi-Ting Jin,<sup>‡</sup> Lu-Yi Huang,<sup>†,||</sup> Guo  
9  
10 Zhang,<sup>‡</sup> Wei Yang,<sup>‡</sup> Kai Chen,<sup>†</sup> Rong Xiang,<sup>#</sup> Chong Chen,<sup>†</sup> Yu-Quan Wei,<sup>†</sup>  
11  
12 Guang-Wen Lu,<sup>†,\*</sup> and Sheng-Yong Yang<sup>†,||,\*</sup>  
13  
14  
15  
16  
17

18 <sup>†</sup>State Key Laboratory of Biotherapy and Cancer Center, West China Hospital,  
19  
20 Sichuan University, and Collaborative Innovation Center for Biotherapy, Chengdu,  
21  
22 610041, PR China.  
23

24  
25 <sup>‡</sup>Key Laboratory of Drug Targeting and Drug Delivery System of Ministry of  
26  
27 Education, West China School of Pharmacy, Sichuan University, Sichuan 610041,  
28  
29 China.  
30  
31

32  
33 <sup>||</sup>School of Chemical Engineering, Sichuan University, and Collaborative Innovation  
34  
35 Center for Biotherapy, Chengdu, 610041, PR China.  
36  
37

38 <sup>#</sup>Department of Clinical Medicine, School of Medicine, Nankai University, Tianjin  
39  
40 300071, China.  
41  
42  
43  
44  
45  
46  
47  
48  
49  
50  
51  
52  
53  
54  
55  
56  
57  
58  
59  
60

## Abstracts

Autophagy inducers represent new promising agents for the treatment of a wide range of medical illnesses. However, safe autophagy inducers for clinical applications are lacking. Inhibition of cdc2-like kinase 1 (CLK1) was recently found to efficiently induce autophagy. Unfortunately, most of the known CLK1 inhibitors have unsatisfactory selectivity. Herein, we report the discovery of a series of new CLK1 inhibitors containing the 1*H*-[1,2,3]triazolo[4,5-*c*]quinoline scaffold. Among them, compound **25** was the most potent and selective, with an IC<sub>50</sub> value of 2 nM against CLK1. The crystal structure of CLK1 complexed with compound **25** was solved, and the potency and kinase selectivity of compound **25** were interpreted. Compound **25** was able to induce autophagy in *in vitro* assays and displayed significant hepatoprotective effects in the acetaminophen (APAP)-induced liver injury mouse model. Collectively, due to its potency and selectivity, compound **25** could be used as a chemical probe or agent in future mechanism-of-action or autophagy-related disease therapy studies.

## 1. INTRODUCTION

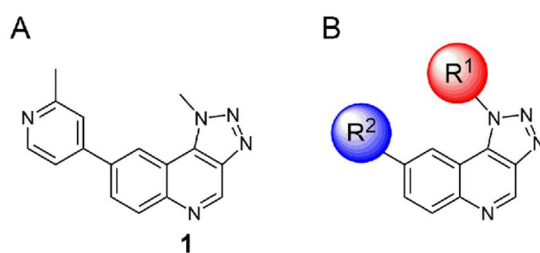
Autophagy is a type of cell “self-eating” phenomenon that can selectively remove damaged or useless organelles and proteins, thus protecting cells from death. Impaired autophagic activity has been linked to a wide range of diseases, including cancer,<sup>1</sup> diabetes,<sup>2,3</sup> neurodegenerative diseases,<sup>4,5</sup> and drug-induced organ injury.<sup>6,7</sup> Autophagy inducers are thus thought of as promising agents for the treatment of these diseases.<sup>8</sup> Currently, only a few autophagy inducers are known.<sup>9</sup> Nevertheless, most of these agents have a wide range of pharmacological activity, which implies a potential risk of toxicity, thus restricting their clinical application.<sup>10</sup> For example, rapamycin, a typical autophagy inducer, could depress the immune system<sup>11,12</sup> and induce insulin resistance.<sup>13,14</sup> Therefore, there is an urgent need to discover more efficient and specific autophagy inducers.

In a recent study, Fant et al.<sup>15</sup> demonstrated that inhibition of cdc2-like kinase 1 (CLK1) could efficiently induce autophagy. The authors also indicated that CLK1 could be a target for the treatment of autophagy-related diseases. To date, a number of CLK1 inhibitors have been reported.<sup>16-21</sup> Despite few inhibitors with definite selectivity, most of the reported CLK1 inhibitors belong to the miscellaneous type, which are associated with unsatisfactory kinase selectivity and are thus not suitable for clinical use due to possible side effects. In particular, these inhibitors, without exception, displayed identical or similar potency against CLK1 and dual-specificity tyrosine-phosphorylation-regulated kinase 1A (DYRK1A).<sup>18,22</sup> DYRK1A is highly homologous in sequence to CLK1,<sup>18</sup> and inhibition of DYRK1A has been shown to

1  
2  
3  
4 pose a potential toxicological risk.<sup>23,24</sup> Therefore, the identification of potent and  
5  
6  
7  
8  
9  
10  
11  
12  
13  
14  
15  
16  
17  
18  
19  
20  
21  
22  
23  
24  
25  
26  
27  
28  
29  
30  
31  
32  
33  
34  
35  
36  
37  
38  
39  
40  
41  
42  
43  
44  
45  
46  
47  
48  
49  
50  
51  
52  
53  
54  
55  
56  
57  
58  
59  
60

pose a potential toxicological risk.<sup>23,24</sup> Therefore, the identification of potent and selective CLK1 inhibitors may have potential clinical application value in the treatment of autophagy-related diseases.

In the effort to seek potent and selective CLK1 inhibitors, we recently obtained a hit compound, 1-methyl-8-(2-methylpyridin-4-yl)-1*H*-[1,2,3]triazolo[4,5-*c*]quinoline (**1**, Figure 1) (for details, see Supporting Information). Compound **1** showed IC<sub>50</sub> values of 139 nM and 420 nM against CLK1 and DYRK1A, respectively. Both the activity and selectivity of this compound were poor and required further optimization. The main purpose of this investigation was to carry out structural optimization and structure-activity relationship (SAR) analyses of compound **1**. We further explored the ability of the most active and selective compound to induce autophagy and explored possible hepatoprotective effects in the acetaminophen (APAP)-induced acute liver injury mouse model.



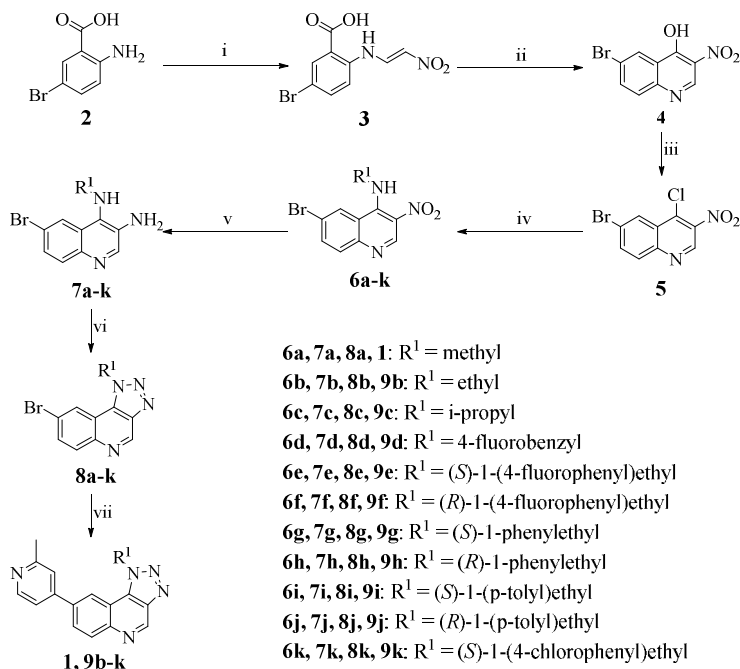
**Figure 1.** (A) The chemical structure of compound **1**. (B) Regions of focus for structural optimization.

## 2. RESULTS AND DISCUSSION

### 2.1 Chemical Syntheses and SAR Analyses

1  
2  
3  
4 The subsequent structural optimization was focused on the R<sup>1</sup> and R<sup>2</sup> regions of  
5  
6 **1** (Figure 1B). In the first step, we fixed R<sup>2</sup> as the original 2-methylpyridin-4-yl group  
7  
8 and varied the R<sup>1</sup> group substituents. The synthetic routes are outlined in Scheme 1.  
9  
10 Briefly, commercially available **2** was reacted with self-prepared 2-nitroacetaldehyde  
11  
12 oxime to obtain **3**, which was dehydrated to yield **4**. Chlorination of **4** afforded the  
13  
14 key intermediate **5**. A nucleophilic substitution reaction between **5** and various  
15  
16 substituted amines yielded intermediates **6a–6k**. The nitro groups of **6a–6k** were  
17  
18 reduced to produce the corresponding amines **7a–7k**, which then underwent a  
19  
20 diazotization and condensation reaction to produce the triazole compounds **8a–8k**.  
21  
22 Final product compounds **1** and **9b–k** were readily obtained through the classic  
23  
24 palladium-catalyzed Suzuki coupling between **8a–8k** and  
25  
26 (2-methylpyridin-4-yl)boronic acid (**29**).  
27  
28  
29  
30  
31  
32  
33  
34  
35

36 **Scheme 1. Synthetic routes of 1 and 9b–9k<sup>a</sup>**  
37  
38  
39  
40  
41  
42  
43  
44  
45  
46  
47  
48  
49  
50  
51  
52  
53  
54  
55  
56  
57  
58  
59  
60



<sup>a</sup>Reagents and conditions: (i) 1). HCl, H<sub>2</sub>O, room temperature (rt); 2). NaOH, H<sub>2</sub>O, 0 °C; 3). HCl, H<sub>2</sub>O, 0 °C; (ii) AcOK, Ac<sub>2</sub>O, 120 °C; (iii) POCl<sub>3</sub>, reflux; (iv) substituted amine, triethylamine, EtOH, reflux; (v) Fe, HAc, 60 °C; (vi) NaNO<sub>2</sub>, AcOH/H<sub>2</sub>O; (vii) **29**, Pd(dppf)Cl<sub>2</sub>, K<sub>2</sub>CO<sub>3</sub>, 1,4-dioxane/H<sub>2</sub>O, 100 °C, 24 h.

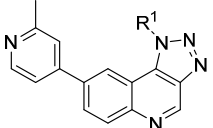
The chemical structures and bioactivities of **9b–9k** and **1** are shown in Table 1.


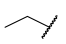
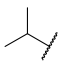
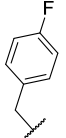
Here, a typical CLK1 inhibitor, (*Z*)-1-(3-ethyl-5-methoxybenzo[*d*]thiazol-2(*3H*)-ylidene)propan-2-one (**30**, called TG003 in literature),<sup>25</sup> was used as a positive control. In addition, we used the ratio of activities against DYRK1A and CLK1 as a selectivity index (SI) to represent the selectivity of compounds, which was primarily based on the following considerations. First, the systematic evaluation of the kinase selectivity must assess the activity of compounds against the entire kinome, which is extremely costly. Second, the amino

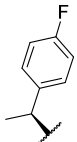
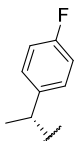
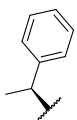
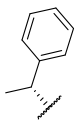
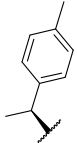
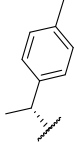
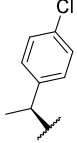


acid sequences of DYRK1A and CLK1 are very similar, with an identity of 70.4%, and the majority of CLK1 inhibitors have comparable potency against DYRK1A. Table 1 shows that the introduction of a benzyl group at the R<sup>1</sup> position benefits the CLK1 activity (**9d** vs **1**, **9b**, and **9c**). Methylation at the benzylic carbon atom leads to chiral derivatives, and the *S*-configuration is more favorable for selectivity (**9e** vs **9f**, **9g** vs **9h**). In addition, the C4 substitution on the phenyl group is sensitive to both potency and selectivity. Compared with the unsubstituted **9g**, compound **9e** with a fluorine (-F) substitution showed the most selectivity, although its potency was marginally decreased. Other substituents, including -methyl (**9i**) and -Cl (**9k**) groups, decreased both the activity and selectivity. To summarize, **9e**, which contains a (*S*)-1-(4-fluorophenyl)ethyl group at the R<sup>1</sup> position, had the highest selectivity and also considerable potency against CLK1.

**Table 1. Structures and bioactivities (IC<sub>50</sub>) of compounds 9b–k and 1<sup>a</sup>**



Cpd.	R <sup>1</sup>	CLK1 [nM]	DYRK1A [nM]	SI <sup>b</sup>
<b>1</b>		139	420	3
<b>9b</b>		66	283	4
<b>9c</b>		64	404	6
<b>9d</b>		7	107	15

1				
2				
3				
4				
5	<b>9e</b>		29	1303
6				45
7				
8				
9				
10	<b>9f</b>		36	194
11				5
12				
13				
14				
15	<b>9g</b>		6	177
16				30
17				
18				
19				
20	<b>9h</b>		24	245
21				10
22				
23				
24				
25	<b>9i</b>		173	1337
26				8
27				
28				
29				
30	<b>9j</b>		34	141
31				4
32				
33				
34				
35	<b>9k</b>		155	1756
36				11
37				
38				
39	<b>30<sup>c</sup></b>		17	71
40				4

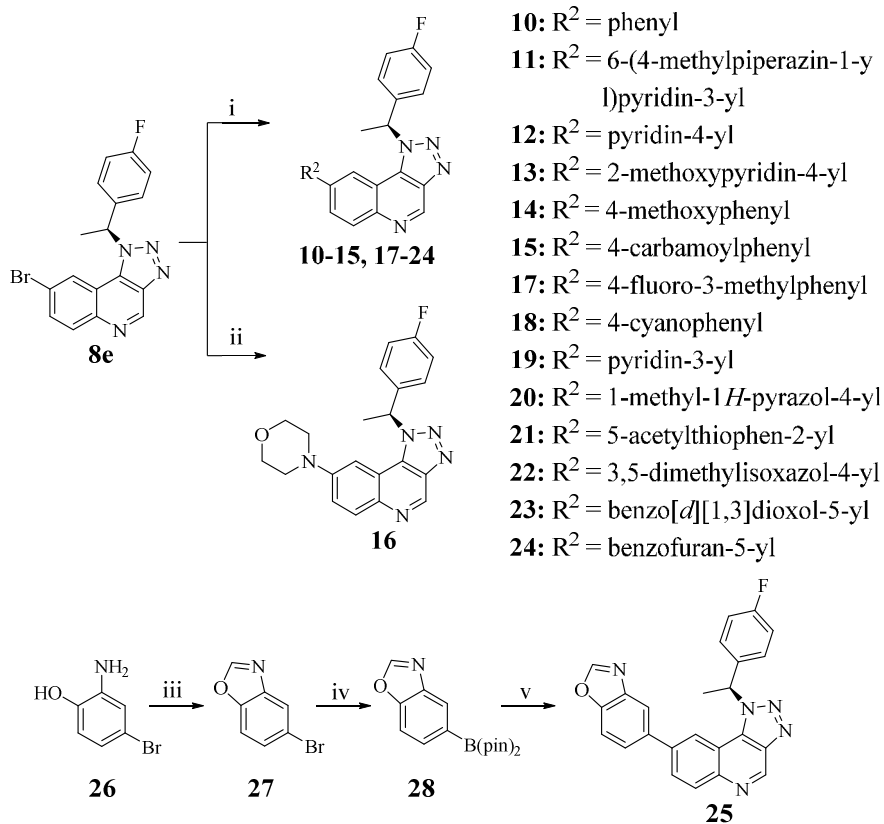
<sup>a</sup>IC<sub>50</sub> values were determined using the KinaseProfiler from Eurofins. The data represent the mean values of two independent experiments; <sup>b</sup>SI denotes the ratio of IC<sub>50</sub> (DYRK1A) to IC<sub>50</sub> (CLK1); <sup>c</sup>positive control; [ATP] = 10 μM.

In the second step, we fixed R<sup>1</sup> as the optimal (*S*)-1-(4-fluorophenyl)ethyl group and altered the R<sup>2</sup> group using different subgroups, including phenyl, pyridyl, substituted phenyl and pyridyl, morpholinyl, five-membered heterocyclic rings, and

1  
2  
3 benzo-fused five-membered heterocyclic rings. Another 16 new compounds (**10–25**)  
4  
5  
6 were then synthesized.  
7

8  
9 The synthetic routes to these compounds are depicted in Scheme 2. Briefly,  
10  
11 Suzuki coupling of **8e** with commercially available aromatic boric acid (or ester)  
12  
13 yielded products **10–15** and **17–24**, and palladium-catalyzed Buchwald coupling  
14  
15 between morpholine and **8e** produced product **16**. By refluxing commercially  
16  
17 available 2-amino-4-bromophenol (**26**) in triethyl orthoformate,  
18  
19 5-bromobenzo[d]oxazole (**27**) could be readily obtained, which subsequently  
20  
21 underwent a Miyaura borylation reaction to yield a benzooxazole-5-boronic acid  
22  
23 pinacol ester (**28**). Then, Suzuki coupling of **28** with **8e** yielded the final product **25**.  
24  
25  
26  
27  
28  
29  
30

31 **Scheme 2. Synthetic routes to 10–25<sup>a</sup>**  
32  
33  
34  
35  
36  
37  
38  
39  
40  
41  
42  
43  
44  
45  
46  
47  
48  
49  
50  
51  
52  
53  
54  
55  
56  
57  
58  
59  
60



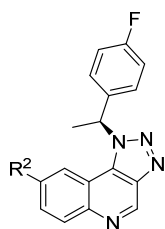
Reagents and conditions: (i) commercially available aromatic boronic acid or boronic acid ester, Pd(dppf)Cl<sub>2</sub>, K<sub>2</sub>CO<sub>3</sub>, 1,4-dioxane/H<sub>2</sub>O, 100 °C, 24 h; (ii) morpholine, Pd<sub>2</sub>(dba)<sub>3</sub>, X-Phos, K<sub>2</sub>CO<sub>3</sub>, t-BuOH, 100 °C, overnight; (iii) triethyl orthoformate, reflux; (iv) bis(pinacolato)diboron, Pd(dppf)Cl<sub>2</sub>, AcOK, 1,4-dioxane, 100 °C; (v) **8e**, Pd(dppf)Cl<sub>2</sub>, K<sub>2</sub>CO<sub>3</sub>, 1,4-dioxane/H<sub>2</sub>O, 100 °C, 24 h.

The chemical structures and bioactivities of compounds **10–25** are shown in Table 2, revealing that substitutions at the R<sup>2</sup> position substantially impacted the activity and selectivity. Compared with **9e**, compounds with bromo (**8e**), phenyl (**10**), substituted phenyl (**14**, **15**, **17**, and **18**), pyridyl (**12**, **19**), substituted pyridyl (**11**, **13**), morpholinyl (**16**), or five-membered heterocyclic (**20–22**) groups at the R<sup>2</sup> position

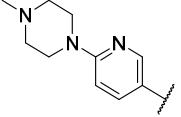
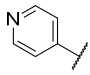
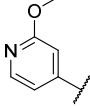
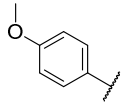
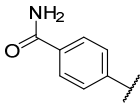
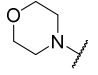
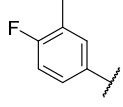
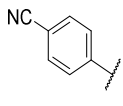
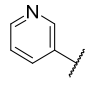
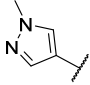
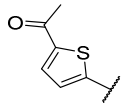
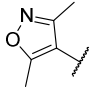
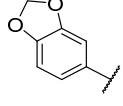
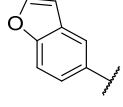
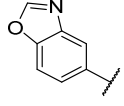
had significantly decreased or completely absent CLK1 activities. Compounds (**23–25**) containing a benzo-fused five-membered heterocyclic group at the R<sup>2</sup> position seemed to have overall improved activity and selectivity. Among them, compound **25** with a benzo[*d*]oxazol-5-yl moiety at the R<sup>2</sup> position exhibited the best performance, with an IC<sub>50</sub> value of 2 nM against CLK1 and 69-fold increased potent activity compared with that of the closely related kinase DYRK1A.

Collectively, compound **25**, which contained (*S*)-1-(4-fluorophenyl)ethyl and benzo[*d*]oxazol-5-yl groups at the R<sup>1</sup> and R<sup>2</sup> positions, respectively, showed the highest potency and selectivity in enzymatic assays. Further in-depth studies were then performed on this compound, including measurement of kinome-wide selectivity, co-crystal structure determination, *in vitro* autophagy-inducing ability examination, and assessment of the *in vivo* effect of liver protection in an acute liver injury model.

**Table 2. Structures and bioactivities (IC<sub>50</sub>) of compounds 10–25<sup>a</sup>**



Cpd.	R <sub>2</sub>	CLK1 [nM]	DYRK1A [nM]	SI <sup>b</sup>
<b>9e</b>		29	1303	45
<b>8e</b>	Br	>10000	>10000	-
<b>10</b>		4985	>10000	2

1					
2					
3					
4					
5	11		>10000	>10000	-
6					
7					
8					
9	12		189	1139	6
10					
11					
12	13		430	2872	7
13					
14					
15	14		439	>10000	23
16					
17					
18	15		186	>10000	54
19					
20					
21	16		529	3360	6
22					
23					
24					
25	17		>10000	>10000	-
26					
27					
28					
29	18		>10000	>10000	-
30					
31					
32					
33	19		>10000	>10000	-
34					
35					
36					
37	20		280	3356	12
38					
39					
40	21		993	>10000	10
41					
42					
43					
44	22		>10000	>10000	-
45					
46					
47					
48	23		18	257	14
49					
50					
51					
52	24		30	1318	44
53					
54					
55	25		2	138	69
56					
57					
58					
59					
60					

1  
2  
3  
4  
5  
6  
7  
8  
9  
10  
11  
12  
13  
14  
15  
16  
17  
18  
19  
20  
21  
22  
23  
24  
25  
26  
27  
28  
29  
30  
31  
32  
33  
34  
35  
36  
37  
38  
39  
40  
41  
42  
43  
44  
45  
46  
47  
48  
49  
50  
51  
52  
53  
54  
55  
56  
57  
58  
59  
60

30 <sup>c</sup>	-	17	71	4
-----------------	---	----	----	---

---

<sup>a</sup>IC<sub>50</sub> values were determined using the KinaseProfiler of Eurofins. The data represent the mean values of two independent experiments; <sup>b</sup>SI denotes the ratio of IC<sub>50</sub> (DYRK1A) to IC<sub>50</sub> (CLK1); <sup>c</sup>positive control; [ATP] = 10 μM.

## 2.2 Kinome-wide Selectivity of **25**

The selectivity of the compounds described above were only for DYRK1A. To examine the kinome-wide selectivity of **25**, we tested the kinase inhibition profiles of this compound against a panel of 357 recombinant human protein kinases. The inhibitory activities of **25** at a fixed concentration of 10 μM were measured first. For kinases with inhibitory rates higher than 50%, further IC<sub>50</sub> values were determined. The results are presented in Supporting Information Table S1. A dendrogram representation of the kinase inhibition by **25** is also shown in Supporting Information Figure S2. As expected, CLK1 was the most potently inhibited kinase (IC<sub>50</sub>: 2 nM). In addition to CLK1, only two kinases had an IC<sub>50</sub> value less than 100 nM, namely, CLK2 (IC<sub>50</sub>: 31 nM) and CLK4 (IC<sub>50</sub>: 8 nM), which are isoforms of CLK1. Except for the CLKs, DYRK1A was the strongest off-target. Furthermore, Supporting Information Table S1 shows that **25** displayed at least 110-fold selectivity toward CLK1 over 351 of the 357 kinases tested (98.32%). Of note is that compound **25** did not show obvious activity against 292 kinases (IC<sub>50</sub> > 10 μM). To the best of our knowledge, **25** is the most potent and selective CLK1 inhibitor identified to date.

### 2.3 Co-crystal Structure of CLK1 Complexed with **25** and the Rationale for its Potency and Selectivity

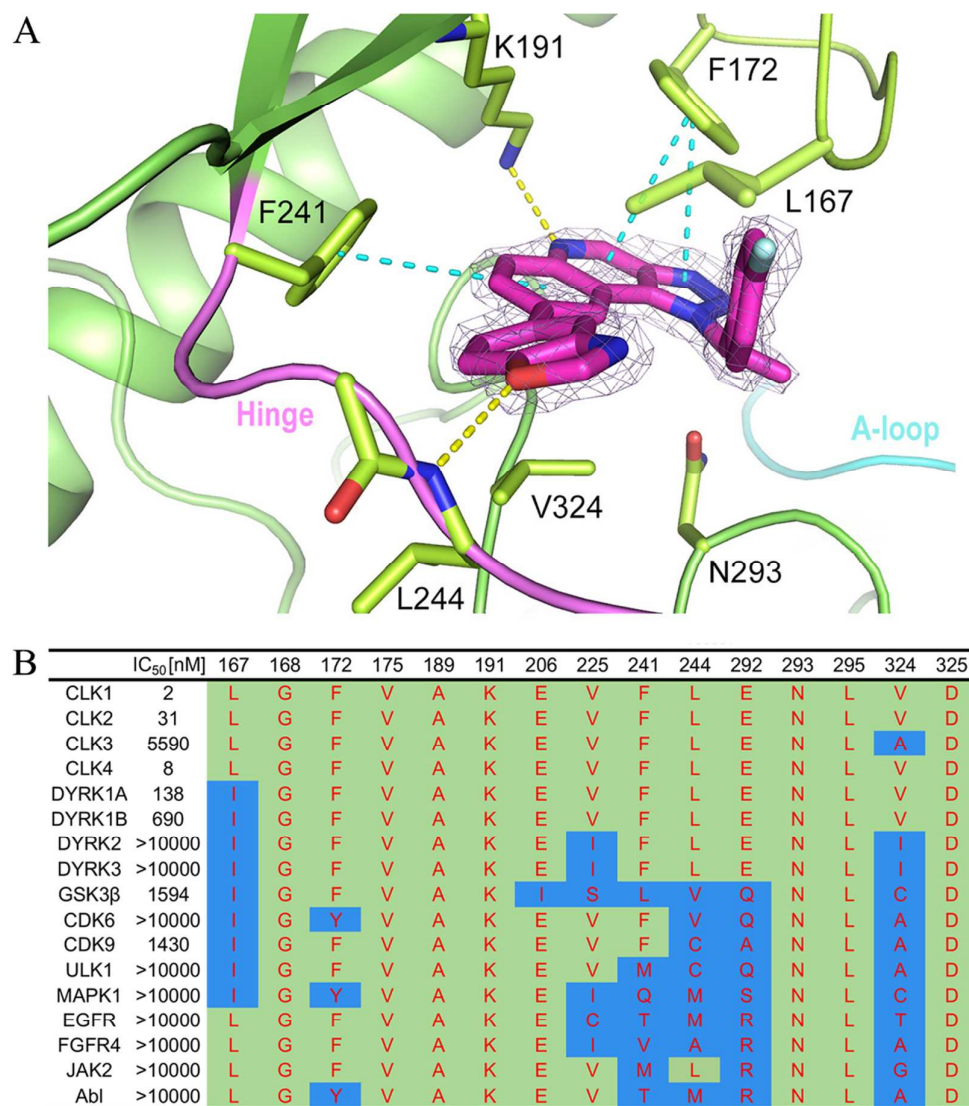
To elucidate the interactions between **25** and CLK1 and the molecular basis of the observed kinase selectivity, we solved the co-crystal structure of the CLK1 kinase domain with **25** at a resolution of 1.9 Å (PDB ID 5X8I). The related data processing and structure refinement statistics are provided in Supporting Information Table S2. Figure 2A displays the key interactions of **25** with CLK1, illustrating that **25** suitably resides in the ATP binding pocket of CLK1, with the benzo[*d*]oxazol-5-yl group pointing toward the hinge region and the triazole moiety of the 1*H*-[1,2,3]triazolo[4,5-*c*]quinoline scaffold pointing toward the solvent area. The quinoline nitrogen and the kinase Lys191 forms an important hydrogen bond. Another important hydrogen bond is formed between the oxazole oxygen atom and Leu244 on the hinge, with the oxazole oxygen atom acting as a hydrogen bond acceptor. The oxazole nitrogen might form some interactions with the hinge region through water-mediated hydrogen-bond-network, which might partially explain the potency increase of benzoxazole **25** compared to benzofuran **24**. In addition, it was also obvious that the tricyclic scaffold of **25** formed a T-shape  $\pi$ - $\pi$  interaction with the benzene ring of CLK1 Phe241 and a  $\pi$ - $\pi$  stacking interaction with the benzene ring of Phe172. Here, it is worth mentioning that quinoline-containing kinase inhibitors usually adopt a canonical hinge binding mode with quinoline making the hinge contacts in the ATP-binding pocket of kinase.<sup>26-28</sup> However, in this case, **25**, which also contains quinoline, adopts an unusual binding mode. Thus, some important



1  
2  
3 interactions indicated above are formed, which could be one of the reasons why the  
4  
5 inhibitor shows such a good selectivity.  
6  
7

8  
9 To understand the preference of **25** in the inhibition of CLK1 over other kinases,  
10  
11 the active amino acids involved in CLK1/**25** interactions were compared between  
12  
13 different kinases via sequence alignment. Figure 2B shows the alignment of the key  
14  
15 residues within 4.5 Å of **25** and CLK1 with the corresponding residues of other  
16  
17 selected kinases (note that numbering is according to CLK1) that include CLK1–4,  
18  
19 DYRK isoforms, and other representative kinases inhibited by **25**, with IC<sub>50</sub> values of  
20  
21 different orders of magnitude. Obviously, the potencies of **25** against different kinases  
22  
23 were strongly dependent on the residues in their active pockets. CLK2/4 had the same  
24  
25 residues as CLK1 in the alignment, explaining why they were potently inhibited by  
26  
27 **25**. The main difference between CLK1/2/4 and CLK3 is the residue 324 (CLK1:  
28  
29 valine; CLK3: alanine). We noted that alanine had a smaller hydrophobic side chain  
30  
31 compared with valine and thus likely weakened the hydrophobic interactions with the  
32  
33 ligand. We hypothesize that this may be the reason why **25** had reduced activity  
34  
35 against CLK3. Similarly, DRYK1A and DYRK1B displayed moderate activity. In  
36  
37 sequence, these two kinases had one residue that differed from CLK1 (CLK1:  
38  
39 LEU167 vs DYRK1A/1B: ILE167). Notably, the substitution of LEU167 (as in  
40  
41 CLK1) with ILE167 (as in DRYK1A/1B) created small amounts of steric hindrance  
42  
43 with **25**, thus requiring a possible conformational adjustment in the residue to properly  
44  
45 accommodate the bound ligand. Accordingly, **25** exhibited decreased activity against  
46  
47 DYRK1A/B compared with CLK1. Finally, other selected kinases all exhibit more  
48  
49  
50  
51  
52  
53  
54  
55  
56  
57  
58  
59  
60

profound residue differences in the ligand binding site, explaining the poor activities of **25** against these proteins.



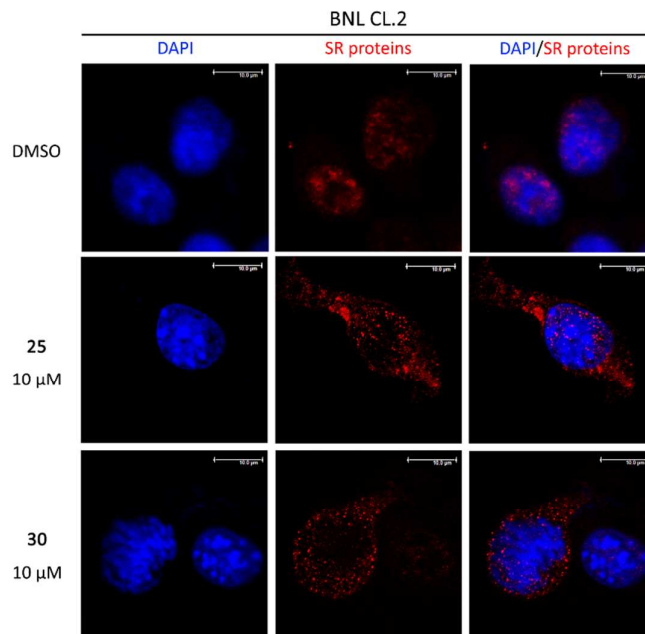
**Figure 2.** The X-ray crystal structure of CLK1 complexed with **25** (PDB ID 5X8I).

(A) Key interactions of **25** with the kinase active site. Yellow and cyan dashed lines indicate hydrogen bonds and  $\pi$ - $\pi$  interactions, respectively. Gray mesh: 2Fo-Fc omitted electron density map contoured at 2.0  $\sigma$ . The images were produced using PyMOL. (B) Multiple-sequence alignment of the selected key residues within the

1  
2  
3  
4 ATP-binding pocket. The residues differing from the corresponding residues of CLK1  
5  
6 are highlighted in blue. Numbering is according to CLK1.  
7  
8  
9

#### 10 11 **2.4 Effects of 25 on the Subcellular Redistribution of Downstream** 12 13 **Serine/Arginine-rich (SR) Proteins in Intact Cells** 14 15

16 SR proteins are typical downstream substrates of CLK1. It has been  
17  
18 demonstrated that activation of CLKs could induce redistribution of SR proteins from  
19  
20 nuclear speckles (stored form) to the nucleoplasm (active form).<sup>29,30</sup> Therefore, to  
21  
22 examine whether **25** can inhibit CLK1 activation in intact cells, we measured the  
23  
24 distribution of SR proteins in cells by immunofluorescence before and after **25**  
25  
26 treatment. Here, BNL CL.2 (mouse embryonic liver cell line) was selected, and three  
27  
28 concentrations (20 nM, 100 nM, and 10  $\mu$ M) of **25** were used. As shown in Figure 3  
29  
30 and Supporting Information Figure S4, **25** treatment indeed led to the redistribution of  
31  
32 SR proteins from the nucleoplasm to nuclear speckles, and the potency showed  
33  
34 significant dose dependency. The same effect was observed for the positive control **30**.  
35  
36 From here, we concluded that **25** could efficiently inhibit the activation of CLK1 in  
37  
38 intact cells.  
39  
40  
41  
42  
43  
44  
45  
46  
47  
48  
49  
50  
51  
52  
53  
54  
55  
56  
57  
58  
59  
60



25  
26  
27  
28  
29  
30  
31  
32  
33  
34  
35  
36  
37  
38  
39

Figure 3. Compound **25** altered the location and redistribution of SR proteins. BNL CL.2 cells treated with **25** (10  $\mu$ M), **30** (10  $\mu$ M) or DMSO (0.1%) for 24 h were fixed and probed with anti-SR proteins antibody (mAb1H4G7). Diffuse staining and typical speckles demonstrated by mAb1H4G7 represent active and stored forms of SR proteins respectively. DAPI was used to dye the nucleus. Scale bar: 10  $\mu$ m.

### 40 41 42 43 44

#### 2.5 Ability of **25** to Induce Autophagy *In Vitro*

45  
46  
47  
48  
49  
50  
51  
52  
53  
54  
55  
56  
57  
58  
59  
60

We next examined the ability of **25** to induce autophagy in BNL CL.2 and SKOV-3 (human ovarian cancer cell line) cells. Compound **30** and the classic autophagy inducer rapamycin were used as positive controls. Western blot assays showed that **25** elevated the expression level of LC3II protein (a marker of autophagosomes<sup>31,32</sup>) as well as the ratio of LC3II to LC3I (a sensitive index of autophagy<sup>33,34</sup>) in a dose-dependent (Figure 4A and 5A) and time-dependent manner (Figure 4B). In accordance with the results of immunoblot assays, confocal

1  
2  
3  
4 microscopy examination showed that **25** increased the number of yellow LC3 puncta  
5  
6 (co-localization of GFP and mRFP signals<sup>35</sup>) in SKOV-3 cells infected with  
7  
8 Ad-mRFP-GFP-LC3 (adenovirus-coding tandem GFP-mRFP-LC3), further  
9  
10 confirming the formation of autophagosomes. The effects of **25** on yellow LC3 puncta  
11  
12 also displayed obvious dose dependency, and a dose of 10  $\mu$ M showed the best  
13  
14 performance (Figure 5B and Supporting Information Figure S5). In addition, in  
15  
16 **25**-treated cells, the number of red LC3 puncta (mRFP signals only<sup>35</sup>) increased  
17  
18 compared with that of DMSO-treated cells, indicating the formation of  
19  
20 autolysosomes. Importantly, **25** stimulated the degradation of SQSTM1/p62 (a marker  
21  
22 of autolysosomes,<sup>36</sup> Figure 4A and Figure 5A) and increased the ratio of red LC3  
23  
24 puncta to yellow LC3 puncta (Figure 5B and Supporting Information Figure S5), both  
25  
26 of which indicated an induction of autophagic flux by **25**. All of these data  
27  
28 demonstrated that **25** could increase the synthesis and clearance of autophagosomes,  
29  
30 and induce autophagy and autophagic flux *in vitro* to levels higher than those resulting  
31  
32 from **30** and rapamycin-induced autophagy, especially in BNL CL.2 cells. In contrast,  
33  
34 compound **18** (negative control), which is inactive against CLK1 ( $IC_{50} > 10 \mu$ M),  
35  
36 could not trigger autophagy even at a concentration of 10  $\mu$ M (Supporting  
37  
38 Information Figure S6).  
39  
40  
41  
42  
43  
44  
45  
46  
47  
48  
49  
50  
51  
52  
53  
54  
55  
56  
57  
58  
59  
60

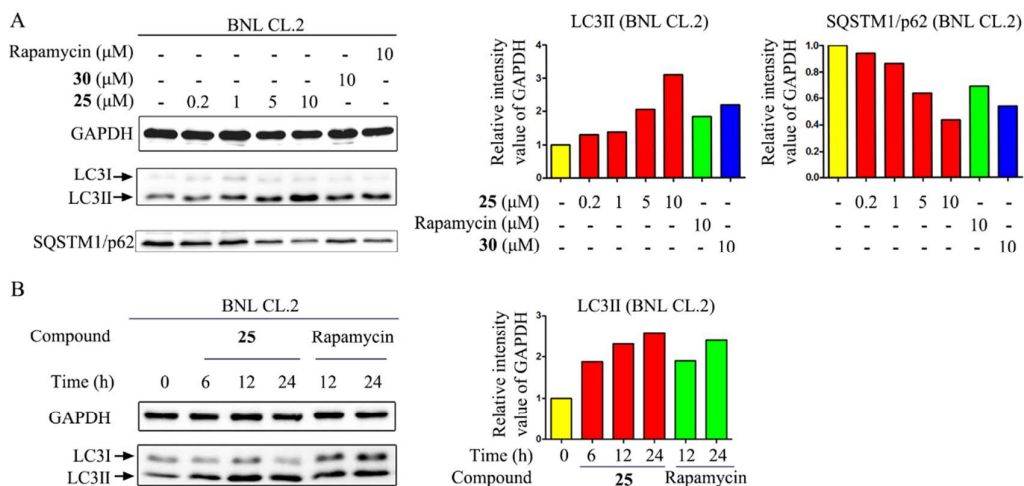
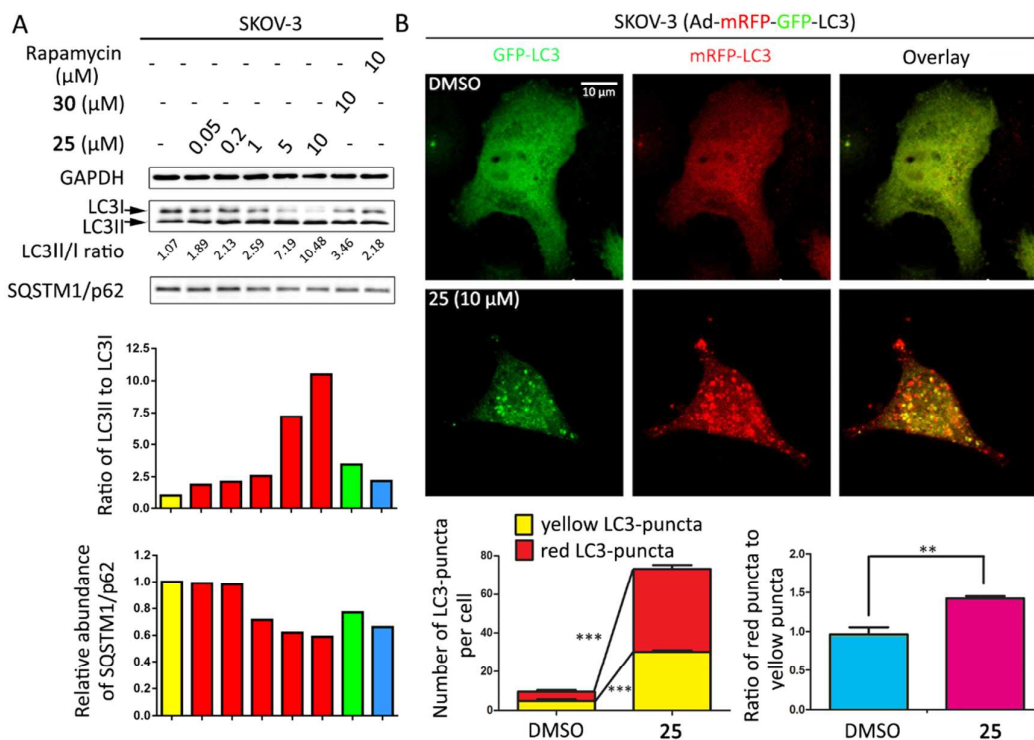


Figure 4. Detection of autophagy and autophagic flux induced by **25** in BNL CL.2 cells. (A) BNL CL.2 cells were treated with rapamycin (positive control), **30** (positive control) and various concentrations of **25** (0.2, 1, 5, and 10  $\mu\text{M}$ ) for 24 h. Then, whole cell lysates were subjected to immunoblot assay to detect LC3 and SQSTM1/p62. Quantification of immunoblots is presented in the right panel. (B) BNL CL.2 cells were treated with **25** or rapamycin, and the level of LC3II protein was detected after 6, 12 and 24 h. Quantification of immunoblots is presented in the right panel.



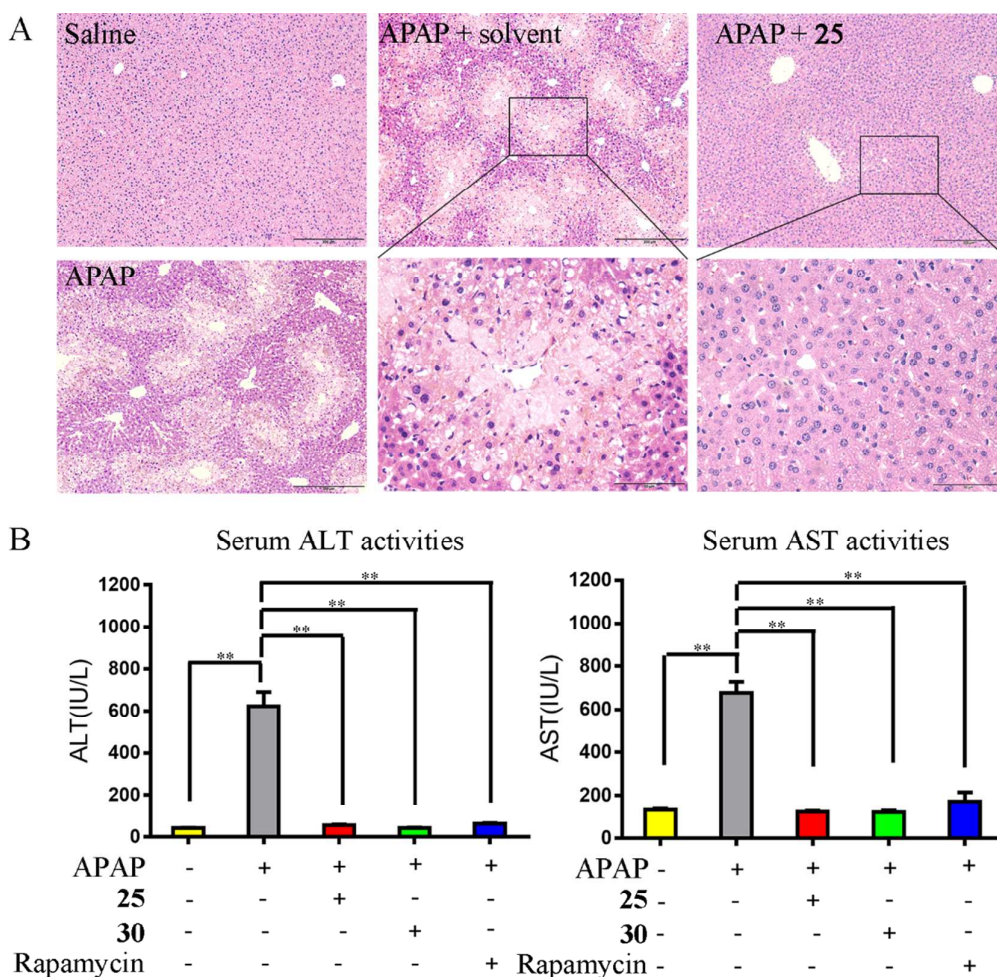
**Figure 5.** Detection of autophagy and autophagic flux induced by **25** in SKOV-3 cells.

(A) SKOV-3 cells were treated with rapamycin (positive control), **30** (positive control) and various concentrations of **25** (0.05, 0.2, 1, 5, and 10  $\mu\text{M}$ ) for 24 h. Then, whole cell lysates were subjected to an immunoblotting assay to detect LC3 and SQSTM1/p62. Immunoblots were quantified as shown below. (B) Ad-mRFP-GFP-LC3-infected SKOV-3 cells were treated with **25** (10  $\mu\text{M}$ ) for 24 h and fixed before examination by confocal microscopy. Representative photographs are presented. Scale bar: 10  $\mu\text{m}$ . Alignment of green and red signals appears yellow. The number of LC3-puncta (mean  $\pm$  SEM) in overlays (Ad-mRFP-GFP-LC3) was quantified and is shown below. More than 80 cells were counted in each individual experiment ( $n = 3$ ). \*\*  $P < 0.01$ , \*\*\*  $P < 0.001$ .

## 2.6 Protective Effect of **25** on APAP-induced Acute Liver Injury

As mentioned above, autophagy inducers may have potential applications in the treatment of relevant diseases. Drug-induced liver injury (DILI) is a major public health concern<sup>37</sup> and accounts for more than 50% of acute liver failure cases. APAP is a widely used antipyretic analgesic drug. However, an overdose of APAP can cause liver injury and even liver failure in humans<sup>38</sup> and is the most frequent cause of acute liver failure, especially in many western countries.<sup>39</sup> Ni et al.<sup>6</sup> found that induction of autophagy by rapamycin inhibited APAP-induced hepatotoxicity, which restricted the necrotic areas and promoted liver regeneration and recovery.<sup>39,40</sup> Herein, the APAP-induced hepatotoxicity mouse model was used to examine the therapeutic effect of **25** *in vivo*. As depicted in Figure 6A, APAP exposure resulted in severe liver injury, and treatment with **25** (ip, 30 mg/kg) imparted a significant hepatoprotective effect. We further detected the levels of the liver enzymes alanine aminotransferase (ALT) and aspartate aminotransferase (AST), high levels of which are considered to be indicators of liver damage. The results showed that treatment with **25** decreased serum ALT and AST levels significantly, such that both marker enzymes returned to normal levels (Figure 6B). Rapamycin and **30** also showed similar hepatoprotective effects in the same model.





35  
36  
37  
38  
39  
40  
41  
42  
43  
44  
45  
46  
47  
48  
49  
50

**Figure 6.** Protective effect of **25** on APAP-induced liver injury in mice. Male C57BL/6 mice were injected (ip) with **25** (30 mg/kg), **30** (30 mg/kg, positive control), rapamycin (30 mg/kg, positive control), or solvent (12.5% ethanol and 12.5% castor oil, 10 ml/kg), immediately followed by APAP (500 mg/kg) injection (ip) for 6 h. (A) Representative photographs of H&E staining are presented. (B) Serum ALT and AST levels were quantified (n = 3 mice). \*\*  $P < 0.01$ .

### 51 3. CONCLUSIONS

52  
53  
54  
55  
56  
57  
58  
59  
60

In summary, a structural optimization of hit compound **1** led to the discovery of a series of new CLK1 inhibitors containing the scaffold 1*H*-[1,2,3]triazolo[4,5-*c*]quinolone. Among them, compound **25** is the most

1  
2  
3  
4 potent and selective. The co-crystal structure of **25** with CLK1 explained its  
5  
6 potent activity and kinase selectivity. This compound also demonstrated an  
7  
8 ability to induce autophagy *in vitro* and had significant hepatoprotective effects  
9  
10 in the APAP-induced liver injury mouse model. A preliminary pharmacokinetic  
11  
12 study in rats showed that **25** had good bioavailability (F = 52.86%, for more  
13  
14 information see Supporting Information Figure S7). All of these results imply  
15  
16 that **25** could be a promising lead compound for the treatment of  
17  
18 autophagy-related diseases. However, the mechanism by which CLK1  
19  
20 inhibition induces autophagy is currently unknown. Further studies, including  
21  
22 an investigation of the mechanism of autophagy induction and preclinical  
23  
24 evaluation in the treatment of autophagy-related diseases, are still underway in  
25  
26 our laboratory.  
27  
28  
29  
30  
31  
32  
33  
34  
35

#### 36 **4. EXPERIMENTAL SECTION**

37  
38 **4.1. Chemistry Methods.** All reagents and solvents were obtained from  
39  
40 commercial suppliers and used without further purification unless otherwise indicated.  
41  
42 Anhydrous solvents were dried and purified by conventional methods prior to use.  
43  
44 Column chromatography was carried out on silica gel (300–400 mesh). All reactions  
45  
46 were monitored by thin-layer chromatography (TLC), and silica gel plates with  
47  
48 fluorescence F-254 were used and visualized with UV light. All of the final  
49  
50 compounds were purified to >95% purity, as determined by high-performance liquid  
51  
52 chromatography (HPLC). HPLC purity analysis was performed on a Waters 2695  
53  
54  
55  
56  
57  
58  
59  
60

1  
2  
3  
4 HPLC system with the use of a Gemini C18 reversed-phase column (4.6 mm  $\Phi$   $\times$  150  
5  
6 mm, particle size: 5  $\mu$ m). The enantiomeric excess (ee) of the products was  
7  
8 determined by HPLC analysis on Waters 2695 system using a Daicel CHIRALPAK<sup>®</sup>  
9  
10 IE chiral column (Lot No. IE00CE-TG015; Part No. 85325; particle size: 5  $\mu$ m;  
11  
12 dimensions: 4.6 mm  $\Phi$   $\times$  150 mm). Optical rotations were measured on a Rudolph  
13  
14 Autopol VI automatic polarimeter, with  $[\alpha]_D^{25}$  values reported in degrees and  
15  
16 concentration (c) reported in g/100 mL. <sup>1</sup>H NMR and <sup>13</sup>C NMR spectra were recorded  
17  
18 on a Bruker AV-400 spectrometer at 400 and 100 MHz, respectively. Coupling  
19  
20 constants (*J*) are expressed in hertz (Hz). Spin multiplicities are described as s  
21  
22 (singlet), d (doublet), t (triplet), dd (doublet of doublet), dt (doublet of triplet), q  
23  
24 (quartet), quint (quintet), brs (broad singlet) and m (multiplet). Chemical shifts ( $\delta$ ) are  
25  
26 listed in parts per million (ppm) relative to tetramethylsilane (TMS) as an internal  
27  
28 standard. For <sup>19</sup>F NMR, chemical shifts are reported on a scale relative to CF<sub>3</sub>COOH  
29  
30 ( $\delta$  -76.55 ppm in DMSO) as an external reference. Low-resolution and high-resolution  
31  
32 ESI-MS readings were recorded on an Agilent 1200-G6410A mass spectrometer.

#### 4.1.1. 1-Methyl-8-(2-methylpyridin-4-yl)-1*H*-[1,2,3]triazolo[4,5-*c*]quinolone

41  
42 **(1)**. Compound **8a** (55 mg, 209.05  $\mu$ mol, 1 equiv), **29** (28.63 mg, 209.05  $\mu$ mol, 1  
43  
44 equiv), Pd(dppf)Cl<sub>2</sub> (15.3 mg, 20.9  $\mu$ mol, 0.1 equiv) and K<sub>2</sub>CO<sub>3</sub> (86.67 mg, 627.14  
45  
46  $\mu$ mol, 3 equiv) were suspended in a mixed solution of 1,4-dioxane and water (4:1).  
47  
48 Under a nitrogen atmosphere, the mixture was stirred at 100 °C for 24 h. The solvent  
49  
50 was evaporated to dryness under reduced pressure to obtain the crude product, which  
51  
52 was purified by flash column chromatography to yield the desired product as a white  
53  
54  
55  
56  
57  
58  
59  
60

1  
2  
3  
4 powder (37.4 mg, 43% yield).  $^1\text{H}$  NMR (400 MHz,  $\text{DMSO-}d_6$ )  $\delta$  9.58 (s, 1H), 8.81 (d,  
5  
6  $J = 1.8$  Hz, 1H), 8.61 (d,  $J = 5.2$  Hz, 1H), 8.37 (d,  $J = 8.7$  Hz, 1H), 8.29 (dd,  $J = 8.7$ ,  
7  
8 1.9 Hz, 1H), 7.86 (s, 1H), 7.79 (dd,  $J = 5.2, 1.5$  Hz, 1H), 4.84 (s, 3H), 2.61 (s, 3H).  
9  
10  $^{13}\text{C}$  NMR (101 MHz,  $\text{DMSO-}d_6$ )  $\delta$  159.28, 150.17, 146.79, 145.77, 145.36, 141.16,  
11  
12 136.93, 133.70, 131.21, 128.72, 121.61, 121.58, 119.59, 116.32, 38.10, 24.70.  
13  
14 ESI-MS  $m/z$  276.2  $[\text{M} + \text{H}]^+$ .  
15  
16  
17

18  
19 **4.1.2. (*E*)-5-Bromo-2-((2-nitrovinyl)amino)benzoic acid (3).** A suspension of  
20  
21 2-amino-5-bromo-benzoic acid (25 g, 115.72 mmol, 1 equiv) in 10:1  $\text{H}_2\text{O}/\text{HCl}$  was  
22  
23 stirred for 8 h and then filtered (solution A). Nitromethane (8.17 g, 133.85 mmol, 1.15  
24  
25 equiv) was added over 10 min to an ice bath-cooled mixture of ice (35 g) and NaOH  
26  
27 (15.3 g, 382.53 mmol, 3.30 equiv). After stirring for 1 h at 0 °C and 1 h at rt, the  
28  
29 solution was added to an ice-bath cooled mixture of ice (28 g) and HCl (37%, 42 mL)  
30  
31 (solution B). Solutions A and B were combined, and the reaction mixture was stirred  
32  
33 overnight at rt. The yellow precipitate was filtered off, washed with  $\text{H}_2\text{O}$  and dried *in*  
34  
35 *vacuo* to yield the crude product, which was used directly in the next step.  
36  
37  
38  
39

40  
41 **4.1.3. 6-Bromo-3-nitroquinolin-4-ol (4).** Compound **3** (5 g, 17.42 mmol, 1  
42  
43 equiv) and potassium acetate (2.05 g, 20.90 mmol, 1.2 equiv) in acetic anhydride were  
44  
45 stirred for 2 h at 120 °C. The precipitate was filtered and washed with acetic acid until  
46  
47 the filtrate was colorless. The precipitate was further washed with water and then  
48  
49 dried to obtain the title compound (2.32 g, two-step yield: 14%).  $^1\text{H}$  NMR (400 MHz,  
50  
51  $\text{DMSO-}d_6$ )  $\delta$  13.21 (s, 1H), 9.24 (s, 1H), 8.32 (d,  $J = 2.3$  Hz, 1H), 7.96 (dd,  $J = 8.8$ ,  
52  
53 2.3 Hz, 1H), 7.71 (d,  $J = 8.8$  Hz, 1H). ESI-MS  $m/z$ : 268.9  $[\text{M} + \text{H}]^+$ .  
54  
55  
56  
57  
58  
59  
60

1  
2  
3  
4       **4.1.4. 6-Bromo-4-chloro-3-nitroquinoline (5).** Compound **4** (2 g, 7.43 mmol)  
5  
6 and POCl<sub>3</sub> were stirred for 4 h at 100 °C. The mixture was cooled to rt and slowly  
7  
8 quenched with ice water. After neutralization with NaHCO<sub>3</sub> (aq.), the aqueous phase  
9  
10 was extracted with ethyl acetate and dried over Na<sub>2</sub>SO<sub>4</sub>. The product was obtained by  
11  
12 evaporation of solution to dryness as a brown solid (2.1 g, 98% yield), which was  
13  
14 used directly in the next step.  
15  
16  
17

18       **4.1.5. 6-Bromo-N-methyl-3-nitroquinolin-4-amine (6a).** To a solution of **5** (1 g,  
19  
20 3.48 mmol, 1 equiv) and triethylamine (703.96 mg, 6.96 mmol, 2 equiv) in EtOH,  
21  
22 methanamine hydrochloride (234.84 mg, 3.48 mmol, 1 equiv) was added slowly at rt.  
23  
24 The resulting mixture was stirred at 60 °C for 4 h. The solution was concentrated *in*  
25  
26 *vacuo* and then poured into water. The precipitate was filtered off and dried to obtain  
27  
28 the desired product as a pale-yellow powder in 89% yield. <sup>1</sup>H NMR (400 MHz,  
29  
30 DMSO-*d*<sub>6</sub>) δ 8.94 (s, 1H), 8.89 (s, 1H), 8.67 (d, *J* = 1.4 Hz, 1H), 7.91 (dd, *J* = 8.8, 1.7  
31  
32 Hz, 1H), 7.78 (d, *J* = 8.8 Hz, 1H), 3.02 (d, *J* = 5.0 Hz, 3H). <sup>13</sup>C NMR (101 MHz,  
33  
34 DMSO-*d*<sub>6</sub>) δ 147.89, 147.33, 147.29, 135.10, 131.84, 126.97, 126.88, 121.73, 119.33,  
35  
36 34.20. ESI-MS *m/z* 281.9 [M + H]<sup>+</sup>.  
37  
38  
39  
40  
41  
42  
43

44       **4.1.6. 6-Bromo-N-methyl-3-nitroquinolin-4-amine (6b).** The title compound  
45  
46 was prepared from **5** (1 g, 3.48 mmol) and commercial available ethanamine  
47  
48 hydrochloride (284 mg, 3.48 mmol) using the procedure described for compound **6a**  
49  
50 in 95% yield as an off-white powder. <sup>1</sup>H NMR (400 MHz, DMSO-*d*<sub>6</sub>) δ 8.97 (d, *J* =  
51  
52 2.6 Hz, 1H), 8.74 (s, 1H), 8.61 (s, 1H), 7.97 – 7.89 (m, 1H), 7.84 – 7.76 (m, 1H), 3.44  
53  
54 – 3.35 (m, 2H), 1.29 (t, *J* = 7.1 Hz, 3H). ESI-MS *m/z* 296.0 [M + H]<sup>+</sup>.  
55  
56  
57  
58  
59  
60

1  
2  
3  
4       **4.1.7. 6-Bromo-*N*-isopropyl-3-nitroquinolin-4-amine (6c).** The title compound  
5  
6 was prepared from **5** (1 g, 3.48 mmol) and commercial available propan-2-amine (298  
7  
8  $\mu\text{L}$ , 3.48 mmol) using the procedure described for compound **6a** in 93% yield as an  
9  
10 off-white powder.  $^1\text{H}$  NMR (400 MHz,  $\text{DMSO-}d_6$ )  $\delta$  8.99 (s, 1H), 8.71 (s, 1H), 8.31 (d,  
11  
12  $J = 7.5$  Hz, 1H), 7.96 (d,  $J = 8.3$  Hz, 1H), 7.83 (d,  $J = 8.8$  Hz, 1H), 4.03 - 3.80 (m, 1H),  
13  
14 1.32 (d,  $J = 6.0$  Hz, 6H). ESI-MS  $m/z$  310.0  $[\text{M} + \text{H}]^+$ .  
15  
16  
17

18  
19       **4.1.8. 6-Bromo-*N*-(4-fluorobenzyl)-3-nitroquinolin-4-amine (6d).** The title  
20  
21 compound was prepared from **5** (750 mg, 2.61 mmol) and commercial available  
22  
23 (4-fluorophenyl)methanamine (327 mg, 2.61 mmol) using the procedure described for  
24  
25 compound **6a** in 91% yield as an off-white powder.  $^1\text{H}$  NMR (400 MHz,  $\text{DMSO-}d_6$ )  $\delta$   
26  
27 9.20 (t,  $J = 5.4$  Hz, 1H), 8.94 (s, 1H), 8.75 (d,  $J = 1.9$  Hz, 1H), 7.96 (dd,  $J = 8.9, 1.9$   
28  
29 Hz, 1H), 7.83 (d,  $J = 8.9$  Hz, 1H), 7.35 (dd,  $J = 8.7, 5.5$  Hz, 2H), 7.23 – 7.10 (m, 2H),  
30  
31 4.70 (d,  $J = 5.7$  Hz, 2H). ESI-MS  $m/z$  376.0  $[\text{M} + \text{H}]^+$ .  
32  
33  
34  
35

36       **4.1.9. (*S*)-6-Bromo-*N*-(1-(4-fluorophenyl)ethyl)-3-nitroquinolin-4-amine (6e).**  
37  
38 The title compound was prepared from **5** (5 g, 17.39 mmol) and commercial available  
39  
40 (*S*)-1-(4-fluorophenyl)ethan-1-amine (2.42 g, 17.39 mmol) using the procedure  
41  
42 described for compound **6a** in 93% yield as an off-white powder.  $^1\text{H}$  NMR (400 MHz,  
43  
44  $\text{DMSO-}d_6$ )  $\delta$  8.96 (s, 1H), 8.86 (d,  $J = 6.5$  Hz, 1H), 8.70 (d,  $J = 1.9$  Hz, 1H), 7.94 (dd,  
45  
46  $J = 8.8, 2.0$  Hz, 1H), 7.81 (d,  $J = 8.8$  Hz, 1H), 7.42 – 7.36 (m, 2H), 7.19 – 7.11 (m,  
47  
48 2H), 5.10 (quint,  $J = 6.6$  Hz, 1H), 1.66 (d,  $J = 6.6$  Hz, 3H).  $^{13}\text{C}$  NMR (101 MHz,  
49  
50  $\text{DMSO-}d_6$ )  $\delta$  163.02, 160.60, 148.01, 147.58, 146.42, 139.45, 139.42, 135.60, 131.93,  
51  
52 128.55, 128.46, 128.34, 128.13, 121.57, 119.58, 116.12, 115.91, 56.60, 25.85.  
53  
54  
55  
56  
57  
58  
59  
60

ESI-MS  $m/z$  390.0  $[M + H]^+$ .

**4.1.10. (R)-6-Bromo-N-(1-(4-fluorophenyl)ethyl)-3-nitroquinolin-4-amine**

**(6f).** The title compound was prepared from **5** (1 g, 3.48 mmol) and commercial available (*R*)-1-(4-fluorophenyl)ethan-1-amine (484 mg, 3.48 mmol) using the procedure described for compound **6a** in 92% yield as an off-white powder.  $^1\text{H}$  NMR (400 MHz,  $\text{DMSO-}d_6$ )  $\delta$  8.96 (s, 1H), 8.86 (d,  $J = 6.7$  Hz, 1H), 8.70 (d,  $J = 1.9$  Hz, 1H), 7.94 (dd,  $J = 8.9, 2.1$  Hz, 1H), 7.81 (d,  $J = 8.8$  Hz, 1H), 7.43 – 7.33 (m, 2H), 7.20 – 7.10 (m, 2H), 5.15 – 5.06 (m, 1H), 1.66 (d,  $J = 6.6$  Hz, 3H). ESI-MS  $m/z$  390.0  $[M + H]^+$ .

**4.1.11. (S)-6-Bromo-3-nitro-N-(1-phenylethyl)quinolin-4-amine (6g).** The title

compound was prepared from **5** (1 g, 3.48 mmol) and commercial available (*S*)-1-phenylethan-1-amine (422 mg, 3.48 mmol) using the procedure described for compound **6a** in 90% yield as an off-white powder.  $^1\text{H}$  NMR (400 MHz,  $\text{DMSO-}d_6$ )  $\delta$  8.98 (s, 1H), 8.70 (d,  $J = 1.7$  Hz, 1H), 7.93 (dd,  $J = 8.9, 2.0$  Hz, 1H), 7.80 (d,  $J = 8.8$  Hz, 1H), 7.40 – 7.29 (m, 2H), 7.28 – 7.20 (m, 1H), 5.13 (quint,  $J = 6.7$  Hz, 1H), 1.67 (d,  $J = 6.6$  Hz, 2H). ESI-MS  $m/z$  372.0  $[M + H]^+$ .

**4.1.12. (R)-6-Bromo-3-nitro-N-(1-phenylethyl)quinolin-4-amine (6h).** The

title compound was prepared from **5** (1 g, 3.48 mmol) and commercial available (*R*)-1-phenylethan-1-amine (422 mg, 3.48 mmol) using the procedure described for compound **6a** in 91% yield as an off-white powder.  $^1\text{H}$  NMR (400 MHz,  $\text{DMSO-}d_6$ )  $\delta$  8.98 (s, 2H), 8.69 (s, 1H), 7.93 (dd,  $J = 8.8, 1.9$  Hz, 1H), 7.80 (d,  $J = 8.8$  Hz, 1H), 7.33 (q,  $J = 8.2$  Hz, 4H), 7.25 (t,  $J = 6.8$  Hz, 1H), 5.23 – 5.07 (m, 1H), 1.67 (d,  $J = 6.6$

1  
2  
3  
4 Hz, 3H). ESI-MS  $m/z$  372.0  $[M + H]^+$ .  
5

6  
7 **4.1.13. (S)-6-Bromo-3-nitro-N-(1-(p-tolyl)ethyl)quinolin-4-amine (6i).** The  
8  
9 title compound was prepared from **5** (1 g, 3.48 mmol) and commercial available  
10  
11 (S)-1-(p-tolyl)ethan-1-amine (470 mg, 3.48 mmol) using the procedure described for  
12  
13 compound **6a** in 90% yield as an off-white powder.  $^1\text{H NMR}$  (400 MHz,  $\text{DMSO-}d_6$ )  $\delta$   
14  
15 8.97 (s, 2H), 8.71 (s, 1H), 7.92 (d,  $J = 8.8$  Hz, 1H), 7.80 (d,  $J = 8.1$  Hz, 1H), 7.22 (d,  $J$   
16  
17 = 8.1 Hz, 2H), 7.12 (d,  $J = 8.0$  Hz, 2H), 5.16 – 5.03 (m, 1H), 2.25 (s, 3H), 1.64 (d,  $J =$   
18  
19 6.6 Hz, 3H). ESI-MS  $m/z$  386.0  $[M + H]^+$ .  
20  
21  
22

23  
24 **4.1.14. (R)-6-Bromo-3-nitro-N-(1-(p-tolyl)ethyl)quinolin-4-amine (6j).** The  
25  
26 title compound was prepared from **5** (1 g, 3.48 mmol) and commercial available  
27  
28 (R)-1-(p-tolyl)ethan-1-amine (470 mg, 3.48 mmol) using the procedure described for  
29  
30 compound **6a** in 92% yield as an off-white powder.  $^1\text{H NMR}$  (400 MHz,  $\text{DMSO-}d_6$ )  $\delta$   
31  
32 8.96 (d,  $J = 9.0$  Hz, 2H), 8.71 (s, 1H), 7.93 (dd,  $J = 8.9, 1.9$  Hz, 1H), 7.80 (d,  $J = 8.8$   
33  
34 Hz, 1H), 7.22 (d,  $J = 8.0$  Hz, 2H), 7.12 (d,  $J = 8.0$  Hz, 2H), 5.09 (quint,  $J = 6.5$  Hz,  
35  
36 1H), 2.25 (s, 3H), 1.64 (d,  $J = 6.6$  Hz, 3H). ESI-MS  $m/z$  386.0  $[M + H]^+$ .  
37  
38  
39  
40

41  
42 **4.1.15. (S)-6-Bromo-N-(1-(4-chlorophenyl)ethyl)-3-nitroquinolin-4-amine**  
43  
44 **(6k).** The title compound was prepared from **5** (900 mg, 3.13 mmol) and commercial  
45  
46 available (S)-1-(4-chlorophenyl)ethan-1-amine (487 mg, 3.13 mmol) using the  
47  
48 procedure described for compound **6a** in 93% yield as an off-white powder.  $^1\text{H NMR}$   
49  
50 (400 MHz,  $\text{DMSO-}d_6$ )  $\delta$  8.96 (s, 1H), 8.83 (d,  $J = 6.2$  Hz, 1H), 8.71 (s, 1H), 7.94 (d,  $J$   
51  
52 = 8.9 Hz, 1H), 7.82 (d,  $J = 8.8$  Hz, 1H), 7.38 (s, 4H), 5.13 – 5.00 (m, 1H), 1.65 (d,  $J =$   
53  
54 6.6 Hz, 3H). ESI-MS  $m/z$  405.9  $[M + H]^+$ .  
55  
56  
57  
58  
59  
60



1  
2  
3  
4  
5  
6  
7  
8  
9  
10  
11  
12  
13  
14  
15  
16  
17  
18  
19  
20  
21  
22  
23  
24  
25  
26  
27  
28  
29  
30  
31  
32  
33  
34  
35  
36  
37  
38  
39  
40  
41  
42  
43  
44  
45  
46  
47  
48  
49  
50  
51  
52  
53  
54  
55  
56  
57  
58  
59  
60

**4.1.16. 8-Bromo-1-methyl-1*H*-[1,2,3]triazolo[4,5-*c*]quinolone (8a).** To a stirred solution of **6a** (1 g, 3.54 mmol, 1 equiv) in AcOH (30 mL), Fe powder (989.82 mg, 17.72 mmol, 5 equiv) was added in several batches at 60 °C. Upon completion of the reaction, the mixture was cooled to rt. The crude product **7a** was used for the next step without further purification.

The reaction flask was transferred into an ice-water bath, and 60 mL of water was poured into the mixture. Concentrated hydrochloric acid was used to adjust the pH to 2–3. Then, a 0.5 mol/L aqueous solution of sodium nitrite (10.64 mL, 5.32 mmol, 1.5 equiv) was added dropwise into the solution under vigorous stirring. The resulting solution was stirred for another 30 min at rt. Then, a large amount of water was added, and the pH was adjusted to 5–6. The aqueous phase was extracted with ethyl acetate. The combined organic phase was separated, dried over anhydrous sodium sulfate and filtered. The filtrate was evaporated to dryness under reduced pressure to yield a solid residue, which was purified by flash column chromatography to yield the desired product as a white powder (730.3 mg, two-step yield: 78%). <sup>1</sup>H NMR (400 MHz, CDCl<sub>3</sub>) δ 9.54 (s, 1H), 8.47 (d, *J* = 2.1 Hz, 1H), 8.21 (d, *J* = 8.9 Hz, 1H), 7.93 (dd, *J* = 8.9, 2.1 Hz, 1H), 4.71 (s, 3H). <sup>13</sup>C NMR (101 MHz, CDCl<sub>3</sub>) δ 145.45, 144.20, 141.28, 133.04, 132.62, 123.94, 121.75, 117.02, 100.00, 37.60. ESI-MS *m/z* 262.9 [M + H]<sup>+</sup>.

**4.1.17. 8-Bromo-1-ethyl-1*H*-[1,2,3]triazolo[4,5-*c*]quinolone (8b).** The title compound was prepared from **6b** (600 mg, 2.03 mmol) in 76% yield as a pale-yellow powder, according to the procedure described for compound **8a**. <sup>1</sup>H NMR (400 MHz,

1  
2  
3  
4 DMSO-*d*<sub>6</sub>)  $\delta$  9.58 (s, 1H), 8.63 (d, *J* = 2.1 Hz, 1H), 8.19 (d, *J* = 8.9 Hz, 1H), 8.05 (dd,  
5  
6 *J* = 8.9, 2.2 Hz, 1H), 5.16 (q, *J* = 7.3 Hz, 2H), 1.63 (t, *J* = 7.3 Hz, 3H). <sup>13</sup>C NMR (101  
7  
8 MHz, DMSO-*d*<sub>6</sub>)  $\delta$  145.78, 144.07, 141.18, 133.23, 132.68, 131.92, 125.34, 121.54,  
9  
10 117.07, 45.92, 15.06. ESI-MS *m/z* 277.0 [M + H]<sup>+</sup>.

11  
12  
13  
14 **4.1.18. 8-Bromo-1-isopropyl-1*H*-[1,2,3]triazolo[4,5-*c*]quinolone (8c).** The title  
15  
16 compound was prepared from **6c** (600 mg, 1.93 mmol) in 75% yield as a white  
17  
18 powder, according to the procedure described for compound **8a**. <sup>1</sup>H NMR (400 MHz,  
19  
20 DMSO-*d*<sub>6</sub>)  $\delta$  9.60 (s, 1H), 8.70 (s, 1H), 8.21 (d, *J* = 8.9 Hz, 1H), 8.06 (dd, *J* = 8.8, 1.3  
21  
22 Hz, 1H), 5.80 – 5.67 (m, 1H), 1.75 (d, *J* = 6.5 Hz, 6H). <sup>13</sup>C NMR (101 MHz,  
23  
24 DMSO-*d*<sub>6</sub>)  $\delta$  145.81, 144.14, 140.87, 133.08, 132.78, 131.58, 125.15, 121.58, 117.15,  
25  
26 53.66, 22.77. ESI-MS *m/z* 291.0 [M + H]<sup>+</sup>.

27  
28  
29  
30  
31 **4.1.19. 8-Bromo-1-(4-fluorobenzyl)-1*H*-[1,2,3]triazolo[4,5-*c*]quinolone (8d).**  
32  
33 The title compound was prepared from **6d** (500 mg, 1.33 mmol) in 73% yield as an  
34  
35 off-white powder, according to the procedure described for compound **8a**. <sup>1</sup>H NMR  
36  
37 (400 MHz, CDCl<sub>3</sub>)  $\delta$  9.58 (s, 1H), 8.28 – 8.13 (m, 2H), 7.86 (dd, *J* = 8.9, 2.1 Hz, 1H),  
38  
39 7.22 (dd, *J* = 8.5, 5.1 Hz, 2H), 7.07 (t, *J* = 8.5 Hz, 2H), 6.21 (s, 2H). <sup>13</sup>C NMR (101  
40  
41 MHz, DMSO-*d*<sub>6</sub>)  $\delta$  163.47, 161.03, 145.85, 144.19, 141.42, 133.34, 132.57, 132.33,  
42  
43 131.77, 131.74, 129.54, 129.45, 125.79, 121.31, 116.60, 116.51, 116.30, 52.69.  
44  
45 ESI-MS *m/z* 357.0 [M + H]<sup>+</sup>.

46  
47  
48  
49  
50  
51 **4.1.20.**

52  
53  
54 **(*S*)-(-)-8-Bromo-1-(1-(4-fluorophenyl)ethyl)-1*H*-[1,2,3]triazolo[4,5-*c*]quinolone**  
55  
56 **(8e).** The title compound was prepared from **6e** (1 g, 2.56 mmol) in 75% yield as a  
57  
58  
59  
60

1  
2  
3  
4 white powder, according to the procedure described for compound **8a**.  $[\alpha]_{\text{D}}^{25} =$   
5  
6  $-220.78$  ( $c = 0.361$ ,  $\text{CH}_3\text{Cl}$ ).  $^1\text{H}$  NMR (400 MHz,  $\text{DMSO-}d_6$ )  $\delta$  9.65 (s, 1H), 8.54 (d,  $J$   
7  
8  $= 2.0$  Hz, 1H), 8.16 (d,  $J = 8.9$  Hz, 1H), 7.99 (dd,  $J = 8.9$ , 1.9 Hz, 1H), 7.35 – 7.24 (m,  
9  
10 2H), 7.19 (t,  $J = 8.8$  Hz, 2H), 6.93 (q,  $J = 6.7$  Hz, 1H), 2.18 (d,  $J = 6.8$  Hz, 3H).  $^{13}\text{C}$   
11  
12 NMR (101 MHz,  $\text{DMSO-}d_6$ )  $\delta$  163.28, 160.85, 145.93, 144.22, 141.24, 137.50,  
13  
14 133.21, 132.68, 132.19, 128.58, 128.49, 125.75, 121.36, 116.73, 116.51, 116.30,  
15  
16 59.85, 23.33. ESI-MS  $m/z$  371.0  $[\text{M} + \text{H}]^+$ .  
17  
18  
19  
20

#### 21 4.1.21.

#### 22 **(R)-(+)-8-Bromo-1-(1-(4-fluorophenyl)ethyl)-1H-[1,2,3]triazolo[4,5-c]quinolone**

23  
24 **(8f)**. The title compound was prepared from **6f** (600 mg, 1.54 mmol) in 73% yield as  
25  
26 an off-white powder, according to the procedure described for compound **8a**.  $[\alpha]_{\text{D}}^{25} =$   
27  
28  $218.22$  ( $c = 0.105$ ,  $\text{CH}_3\text{Cl}$ ).  $^1\text{H}$  NMR (400 MHz,  $\text{DMSO-}d_6$ )  $\delta$  9.65 (s, 1H), 8.54 (d,  $J$   
29  
30  $= 2.0$  Hz, 1H), 8.16 (d,  $J = 8.9$  Hz, 1H), 7.99 (dd,  $J = 8.9$ , 1.8 Hz, 1H), 7.33 – 7.25 (m,  
31  
32 2H), 7.19 (t,  $J = 8.8$  Hz, 2H), 6.93 (q,  $J = 6.8$  Hz, 1H), 2.17 (d,  $J = 6.8$  Hz, 3H).  $^{13}\text{C}$   
33  
34 NMR (101 MHz,  $\text{DMSO-}d_6$ )  $\delta$  163.28, 160.85, 145.90, 144.20, 141.22, 137.49,  
35  
36 137.46, 133.17, 132.65, 132.17, 128.57, 128.49, 125.73, 121.35, 116.71, 116.50,  
37  
38 116.29, 59.86, 23.33. ESI-MS  $m/z$  371.0  $[\text{M} + \text{H}]^+$ .  
39  
40  
41  
42  
43  
44  
45

#### 46 4.1.22. **(S)-8-Bromo-1-(1-phenylethyl)-1H-[1,2,3]triazolo[4,5-c]quinolone**

47  
48 **(8g)**. The title compound was prepared from **6g** (600 mg, 1.61 mmol) in 69% yield as  
49  
50 an off-white powder, according to the procedure described for compound **8a**.  $^1\text{H}$  NMR  
51  
52 (400 MHz,  $\text{DMSO-}d_6$ )  $\delta$  9.65 (s, 1H), 8.50 (d,  $J = 1.8$  Hz, 1H), 8.15 (d,  $J = 8.8$  Hz,  
53  
54 1H), 7.97 (d,  $J = 8.9$  Hz, 1H), 7.35 (t,  $J = 7.4$  Hz, 2H), 7.27 (t,  $J = 7.3$  Hz, 1H), 7.24 –  
55  
56  
57  
58  
59  
60

1  
2  
3  
4 7.16 (m, 2H), 6.89 (q,  $J = 6.7$  Hz, 1H), 2.19 (d,  $J = 6.8$  Hz, 3H).  $^{13}\text{C}$  NMR (101 MHz,  
5  
6 DMSO- $d_6$ )  $\delta$  145.91, 144.17, 141.35, 141.25, 133.11, 132.61, 132.25, 129.58, 128.51,  
7  
8 126.17, 125.87, 121.26, 116.73, 60.58, 23.36. ESI-MS  $m/z$  353.0  $[\text{M} + \text{H}]^+$ .

9  
10  
11 **4.1.23. (R)-8-Bromo-1-(1-phenylethyl)-1H-[1,2,3]triazolo[4,5-c]quinolone**

12 **(8h)**. The title compound was prepared from **6h** (600 mg, 1.61 mmol) in 79% yield as  
13  
14 a pale-yellow powder, according to the procedure described for compound **8a**.  $^1\text{H}$   
15  
16 NMR (400 MHz, DMSO- $d_6$ )  $\delta$  9.65 (s, 1H), 8.51 (d,  $J = 2.1$  Hz, 1H), 8.14 (d,  $J = 8.9$   
17  
18 Hz, 1H), 7.96 (dd,  $J = 8.9, 2.1$  Hz, 1H), 7.36 (dd,  $J = 10.1, 4.6$  Hz, 2H), 7.32 – 7.25  
19  
20 (m, 1H), 7.25 – 7.16 (m, 2H), 6.89 (q,  $J = 6.7$  Hz, 1H), 2.20 (d,  $J = 6.8$  Hz, 3H).  $^{13}\text{C}$   
21  
22 NMR (101 MHz, DMSO- $d_6$ )  $\delta$  145.91, 144.18, 141.34, 141.25, 133.11, 132.60,  
23  
24 132.25, 129.58, 128.51, 126.17, 125.87, 121.25, 116.73, 60.59, 23.35. ESI-MS  $m/z$   
25  
26 353.0  $[\text{M} + \text{H}]^+$ .

27  
28  
29 **4.1.24. (S)-8-Bromo-1-(1-(p-tolyl)ethyl)-1H-[1,2,3]triazolo[4,5-c]quinolone**

30  
31 **(8i)**. The title compound was prepared from **6i** (500 mg, 1.29 mmol) in 77% yield as  
32  
33 an off-white powder, according to the procedure described for compound **8a**.  $^1\text{H}$  NMR  
34  
35 (400 MHz,  $\text{CDCl}_3$ )  $\delta$  9.57 (s, 1H), 8.28 (d,  $J = 2.1$  Hz, 1H), 8.13 (d,  $J = 8.9$  Hz, 1H),  
36  
37 7.81 (dd,  $J = 8.9, 2.1$  Hz, 1H), 7.16 (d,  $J = 8.1$  Hz, 2H), 7.11 (d,  $J = 8.2$  Hz, 2H), 6.34  
38  
39 (q,  $J = 6.8$  Hz, 1H), 2.29 (d,  $J = 6.8$  Hz, 6H), 2.30 (s, 3H).  $^{13}\text{C}$  NMR (101 MHz,  
40  
41 DMSO- $d_6$ )  $\delta$  145.92, 144.17, 141.24, 138.41, 137.82, 133.11, 132.61, 132.20, 130.09,  
42  
43 126.08, 125.93, 121.26, 116.75, 60.42, 23.41, 21.03. ESI-MS  $m/z$  367.0  $[\text{M} + \text{H}]^+$ .

44  
45  
46 **4.1.25. (R)-8-Bromo-1-(1-(p-tolyl)ethyl)-1H-[1,2,3]triazolo[4,5-c]quinolone**

47  
48  
49 **(8j)**. The title compound was prepared from **6j** (600 mg, 1.55 mmol) in 74% yield as  
50  
51  
52  
53  
54  
55  
56  
57  
58  
59  
60

1  
2  
3  
4 an off-white powder, according to the procedure described for compound **8a**. <sup>1</sup>H NMR  
5  
6 (400 MHz, DMSO-*d*<sub>6</sub>) δ 9.64 (s, 1H), 8.52 (d, *J* = 2.1 Hz, 1H), 8.15 (d, *J* = 8.9 Hz,  
7  
8 1H), 7.97 (dd, *J* = 8.9, 2.1 Hz, 1H), 7.14 (d, *J* = 8.1 Hz, 2H), 7.09 (d, *J* = 8.2 Hz, 2H),  
9  
10 6.84 (q, *J* = 6.7 Hz, 1H), 2.22 (s, 3H), 2.16 (d, *J* = 6.8 Hz, 3H). <sup>13</sup>C NMR (101 MHz,  
11  
12 DMSO-*d*<sub>6</sub>) δ 145.92, 144.17, 141.24, 138.41, 137.82, 133.11, 132.61, 132.20, 130.10,  
13  
14 126.08, 125.93, 121.26, 116.76, 60.42, 23.41, 21.03. ESI-MS *m/z* 367.0 [M + H]<sup>+</sup>.  
15  
16  
17

#### 18 19 4.1.26.

#### 20 21 **(S)-8-Bromo-1-(1-(4-chlorophenyl)ethyl)-1*H*-[1,2,3]triazolo[4,5-*c*]quinolone (8k).**

22  
23 The title compound was prepared from **6k** (500 mg, 1.23 mmol) in 77% yield as an  
24  
25 off-white powder, according to the procedure described for compound **8a**. <sup>1</sup>H NMR  
26  
27 (400 MHz, CDCl<sub>3</sub>) δ 9.58 (s, 1H), 8.23 (d, *J* = 1.8 Hz, 1H), 8.17 (dd, *J* = 8.8, 3.7 Hz,  
28  
29 1H), 7.89 – 7.79 (m, 1H), 7.39 – 7.31 (m, 2H), 7.17 (d, *J* = 8.5 Hz, 2H), 6.36 (q, *J* =  
30  
31 6.9 Hz, 1H), 2.32 (d, *J* = 7.0 Hz, 3H). <sup>13</sup>C NMR (101 MHz, DMSO-*d*<sub>6</sub>) δ 145.90,  
32  
33 144.21, 141.22, 140.25, 133.20, 133.17, 132.66, 132.21, 129.55, 128.28, 125.67,  
34  
35 121.38, 116.69, 59.84, 23.15. ESI-MS *m/z* 386.9 [M + H]<sup>+</sup>.  
36  
37  
38  
39  
40

#### 41 42 4.1.27. 1-Ethyl-8-(2-methylpyridin-4-yl)-1*H*-[1,2,3]triazolo[4,5-*c*]quinoline

43  
44 **(9b)**. The title compound was prepared from **8b** (50 mg, 180 μmol) and **29** (25 mg,  
45  
46 180 μmol) using the procedure described for compound **1** in 76% yield as an off-white  
47  
48 powder. <sup>1</sup>H NMR (400 MHz, DMSO-*d*<sub>6</sub>) δ 9.58 (s, 1H), 8.68 (d, *J* = 1.5 Hz, 1H), 8.61  
49  
50 (d, *J* = 5.2 Hz, 1H), 8.36 (d, *J* = 8.7 Hz, 1H), 8.26 (dd, *J* = 8.7, 1.7 Hz, 1H), 7.80 (s,  
51  
52 1H), 7.75 (d, *J* = 5.1 Hz, 1H), 5.27 (q, *J* = 7.2 Hz, 2H), 2.61 (s, 3H), 1.69 (t, *J* = 7.2  
53  
54 Hz, 3H). <sup>13</sup>C NMR (101 MHz, DMSO-*d*<sub>6</sub>) δ 159.28, 150.18, 146.78, 145.85, 145.41,  
55  
56  
57  
58  
59  
60

1  
2  
3  
4 141.25, 137.29, 132.83, 131.43, 128.75, 121.66, 121.22, 119.62, 115.95, 46.03, 24.70,  
5  
6 15.02. ESI-MS  $m/z$  290.1  $[M + H]^+$ .  
7

#### 8 9 4.1.28.

10  
11 **1-Isopropyl-8-(2-methylpyridin-4-yl)-1H-[1,2,3]triazolo[4,5-c]quinolone (9c).** The  
12  
13 title compound was prepared from **8c** (50 mg, 172  $\mu\text{mol}$ ) and **29** (24 mg, 172  $\mu\text{mol}$ )  
14  
15 using the procedure described for compound **1** in 80% yield as an off-white powder.  
16  
17  $^1\text{H}$  NMR (400 MHz,  $\text{CDCl}_3$ )  $\delta$  9.59 (s, 1H), 8.67 (d,  $J = 5.2$  Hz, 1H), 8.49 (d,  $J = 1.9$   
18  
19 Hz, 1H), 8.45 (d,  $J = 8.7$  Hz, 1H), 8.06 (dd,  $J = 8.7, 2.0$  Hz, 1H), 7.49 (s, 1H), 7.44  
20  
21 (dd,  $J = 5.2, 1.4$  Hz, 1H), 5.53 (m, 1H), 2.71 (s, 3H), 1.96 (d,  $J = 6.6$  Hz, 6H).  $^{13}\text{C}$   
22  
23 NMR (101 MHz,  $\text{DMSO}-d_6$ )  $\delta$  159.27, 150.19, 146.87, 145.99, 145.54, 141.02,  
24  
25 137.38, 132.58, 131.62, 128.73, 121.73, 121.16, 119.70, 116.12, 53.77, 24.74, 22.77.  
26  
27 ESI-MS  $m/z$  304.2  $[M + H]^+$ .  
28  
29  
30  
31  
32

#### 33 34 4.1.29.

35  
36 **1-(4-Fluorobenzyl)-8-(2-methylpyridin-4-yl)-1H-[1,2,3]triazolo[4,5-c]quinolone**  
37  
38 **(9d).** The title compound was prepared from **8d** (50 mg, 140  $\mu\text{mol}$ ) and **29** (19 mg,  
39  
40 140  $\mu\text{mol}$ ) using the procedure described for compound **1** in 84% yield as a  
41  
42 pale-yellow powder.  $^1\text{H}$  NMR (400 MHz,  $\text{DMSO}-d_6$ )  $\delta$  9.67 (s, 1H), 8.60 (d,  $J = 5.2$   
43  
44 Hz, 1H), 8.45 (s, 1H), 8.34 (d,  $J = 8.7$  Hz, 1H), 8.24 (d,  $J = 8.6$  Hz, 1H), 7.54 (d,  $J =$   
45  
46 4.9 Hz, 1H), 7.49 (s, 1H), 7.38 – 7.29 (m, 2H), 7.23 (t,  $J = 8.8$  Hz, 2H), 6.57 (s, 2H),  
47  
48 2.60 (s, 3H).  $^{13}\text{C}$  NMR (101 MHz,  $\text{DMSO}-d_6$ )  $\delta$  162.95, 160.52, 158.76, 149.70,  
49  
50 145.94, 145.48, 145.06, 141.07, 136.42, 132.77, 131.57, 130.82, 128.82, 128.74,  
51  
52 128.29, 121.36, 120.87, 118.81, 116.10, 115.89, 115.02, 52.29, 24.18. ESI-MS  $m/z$   
53  
54  
55  
56  
57  
58  
59  
60

370.1 [M + H]<sup>+</sup>.

#### 4.1.30.

**(S)-(-)-1-(1-(4-Fluorophenyl)ethyl)-8-(2-methylpyridin-4-yl)-1H-[1,2,3]triazolo[4,5-c]quinolone (9e).** The title compound was prepared from **8e** (50 mg, 135 μmol) and **29** (19 mg, 135 μmol) using the procedure described for compound **1** in 85% yield as a white powder.  $[\alpha]_D^{25} = -188.72$  (c = 0.133, CH<sub>3</sub>Cl). <sup>1</sup>H NMR (400 MHz, DMSO-*d*<sub>6</sub>) δ 9.67 (s, 1H), 8.63 (d, *J* = 5.1 Hz, 1H), 8.52 (d, *J* = 1.8 Hz, 1H), 8.33 (d, *J* = 8.7 Hz, 1H), 8.22 (dd, *J* = 8.7, 2.0 Hz, 1H), 7.60 – 7.57 (m, 1H), 7.56 (s, 1H), 7.38 – 7.30 (m, 2H), 7.26 – 7.17 (m, 2H), 7.05 (q, *J* = 6.7 Hz, 1H), 2.64 (s, 3H), 2.23 (d, *J* = 6.8 Hz, 3H). <sup>13</sup>C NMR (101 MHz, DMSO-*d*<sub>6</sub>) δ 163.26, 160.83, 159.28, 150.20, 146.46, 146.04, 145.59, 141.40, 137.97, 137.94, 136.89, 133.18, 131.43, 128.62, 128.41, 128.32, 121.74, 121.38, 119.34, 116.63, 116.41, 115.65, 60.13, 24.70, 23.59. ESI-MS *m/z*: 384.1 [M + H]<sup>+</sup>. HPLC analysis (H<sub>2</sub>O/MeCN = 4/6, *t*<sub>R</sub> = 18.09 min)

#### 4.1.31.

**(R)-(+)-1-(1-(4-Fluorophenyl)ethyl)-8-(2-methylpyridin-4-yl)-1H-[1,2,3]triazolo[4,5-c]quinolone (9f).** The title compound was prepared from **8f** (50 mg, 135 μmol) and **29** (19 mg, 135 μmol) using the procedure described for compound **1** in 87% yield as an off-white powder.  $[\alpha]_D^{25} = 187.85$  (c = 0.109, CH<sub>3</sub>Cl). <sup>1</sup>H NMR (400 MHz, DMSO-*d*<sub>6</sub>) δ 9.67 (s, 1H), 8.62 (d, *J* = 5.2 Hz, 1H), 8.51 (d, *J* = 1.6 Hz, 1H), 8.34 (d, *J* = 8.7 Hz, 1H), 8.23 (d, *J* = 8.7 Hz, 1H), 7.58 (d, *J* = 5.2 Hz, 1H), 7.56 (s, 1H), 7.37 – 7.28 (m, 2H), 7.21 (t, *J* = 8.8 Hz, 2H), 7.04 (q, *J* = 6.7 Hz, 1H), 2.63 (s, 3H), 2.22 (d, *J* = 6.8 Hz, 3H). <sup>13</sup>C NMR (101 MHz, DMSO-*d*<sub>6</sub>) δ 162.75, 160.32, 158.79, 149.71,

1  
2  
3  
4 145.96, 145.56, 145.10, 140.91, 137.46, 137.43, 136.41, 132.69, 130.95, 128.14,  
5  
6 127.90, 127.82, 121.25, 120.88, 118.85, 116.12, 115.91, 115.16, 59.62, 24.20, 23.88,  
7  
8 23.09. ESI-MS  $m/z$  384.4  $[M + H]^+$ .

#### 11 4.1.32.

#### 14 (S)-(-)-8-(2-Methylpyridin-4-yl)-1-(1-phenylethyl)-1*H*-[1,2,3]triazolo[4,5-*c*]quinol

15 **one (9g)**. The title compound was prepared from **8g** (55 mg, 156  $\mu\text{mol}$ ) and **29** (21 mg,  
16 156  $\mu\text{mol}$ ) using the procedure described for compound **1** in 91% yield as an off-white  
17 powder.  $[\alpha]_D^{25} = -178.67$  ( $c = 0.147$ ,  $\text{CH}_3\text{Cl}$ ).  $^1\text{H}$  NMR (400 MHz,  $\text{DMSO-}d_6$ )  $\delta$  9.67  
18 (s, 1H), 8.60 (d,  $J = 5.2$  Hz, 1H), 8.49 (d,  $J = 1.7$  Hz, 1H), 8.32 (d,  $J = 8.6$  Hz, 1H),  
19 8.21 (d,  $J = 8.7$  Hz, 1H), 7.53 (d,  $J = 5.3$  Hz, 1H), 7.52 (s, 1H), 7.37 (t,  $J = 7.5$  Hz,  
20 2H), 7.29 (d,  $J = 7.3$  Hz, 1H), 7.27 – 7.22 (m, 2H), 7.01 (q,  $J = 6.6$  Hz, 1H), 2.62 (s,  
21 3H), 2.23 (d,  $J = 6.8$  Hz, 3H).  $^{13}\text{C}$  NMR (101 MHz,  $\text{DMSO-}d_6$ )  $\delta$  159.25, 150.17,  
22 146.48, 146.07, 145.57, 141.83, 141.43, 136.78, 133.26, 131.38, 129.70, 128.55,  
23 128.51, 126.06, 121.97, 121.34, 119.33, 115.68, 60.82, 24.69, 23.60. ESI-MS  $m/z$   
24 366.2  $[M + H]^+$ .

#### 41 4.1.33.

#### 44 (R)-(+)-8-(2-Methylpyridin-4-yl)-1-(1-phenylethyl)-1*H*-[1,2,3]triazolo[4,5-*c*]quino

45 **lone (9h)**. The title compound was prepared from **8h** (50 mg, 142  $\mu\text{mol}$ ) and **29** (19  
46 mg, 142  $\mu\text{mol}$ ) using the procedure described for compound **1** in 92% yield as a white  
47 powder.  $[\alpha]_D^{25} = 180.43$  ( $c = 0.111$ ,  $\text{CH}_3\text{Cl}$ ).  $^1\text{H}$  NMR (400 MHz,  $\text{DMSO-}d_6$ )  $\delta$  9.67 (s,  
48 1H), 8.60 (d,  $J = 5.1$  Hz, 1H), 8.49 (s, 1H), 8.32 (d,  $J = 8.7$  Hz, 1H), 8.20 (dd,  $J = 8.7$ ,  
49 1.6 Hz, 1H), 7.53 (d,  $J = 5.6$  Hz, 1H), 7.52 (s, 1H), 7.37 (t,  $J = 7.5$  Hz, 2H), 7.29 (d,  $J$   
50  
51  
52  
53  
54  
55  
56  
57  
58  
59  
60



1  
2  
3  
4 = 7.2 Hz, 1H), 7.25 (d,  $J = 7.5$  Hz, 2H), 7.01 (q,  $J = 6.7$  Hz, 1H), 2.62 (s, 3H), 2.23 (d,  
5  
6  $J = 6.8$  Hz, 3H).  $^{13}\text{C}$  NMR (101 MHz, DMSO- $d_6$ )  $\delta$  159.25, 150.17, 146.48, 146.07,  
7  
8 145.57, 141.83, 141.43, 136.78, 133.26, 131.38, 129.70, 128.55, 128.51, 126.06,  
9  
10 121.97, 121.34, 119.33, 115.68, 60.82, 24.69, 23.60. ESI-MS  $m/z$  366.2  $[\text{M} + \text{H}]^+$ .

#### 13 14 4.1.34.

15  
16 **(S)-(-)-8-(2-Methylpyridin-4-yl)-1-(1-(p-tolyl)ethyl)-1H-[1,2,3]triazolo[4,5-c]quino**  
17  
18 **lone (9i).** The title compound was prepared from **8i** (52 mg, 142  $\mu\text{mol}$ ) and **29** (20 mg,  
19  
20 142  $\mu\text{mol}$ ) using the procedure described for compound **1** in 91% yield as an off-white  
21  
22 powder.  $[\alpha]_{\text{D}}^{25} = -228.32$  ( $c = 0.113$ ,  $\text{CH}_3\text{Cl}$ ).  $^1\text{H}$  NMR (400 MHz, DMSO- $d_6$ )  $\delta$  9.66  
23  
24 (s, 1H), 8.61 (d,  $J = 5.2$  Hz, 1H), 8.51 (d,  $J = 1.8$  Hz, 1H), 8.32 (d,  $J = 8.7$  Hz, 1H),  
25  
26 8.21 (dd,  $J = 8.7, 2.0$  Hz, 1H), 7.56 (d,  $J = 5.2$  Hz, 1H), 7.53 (s, 1H), 7.15 (q,  $J = 8.2$   
27  
28 Hz, 4H), 6.96 (q,  $J = 6.7$  Hz, 1H), 2.63 (s, 3H), 2.21 (s, 3H), 2.20 (d,  $J = 6.8$  Hz, 3H).  
29  
30  $^{13}\text{C}$  NMR (101 MHz, DMSO- $d_6$ )  $\delta$  158.76, 149.69, 146.01, 145.56, 145.07, 140.91,  
31  
32 138.36, 137.32, 136.28, 132.71, 130.87, 129.70, 128.05, 125.47, 121.52, 120.87,  
33  
34 118.85, 115.20, 60.15, 24.18, 23.13, 20.51. ESI-MS  $m/z$  380.2  $[\text{M} + \text{H}]^+$ .

#### 35 36 4.1.35.

37  
38 **(R)-(+)-8-(2-Methylpyridin-4-yl)-1-(1-(p-tolyl)ethyl)-1H-[1,2,3]triazolo[4,5-c]quin**  
39  
40 **olone (9j).** The title compound was prepared from **8j** (50 mg, 136  $\mu\text{mol}$ ) and **29** (19  
41  
42 mg, 136  $\mu\text{mol}$ ) using the procedure described for compound **1** in 90% yield as a  
43  
44 yellow powder.  $[\alpha]_{\text{D}}^{25} = 227.81$  ( $c = 0.119$ ,  $\text{CH}_3\text{Cl}$ ).  $^1\text{H}$  NMR (400 MHz, DMSO- $d_6$ )  $\delta$   
45  
46 9.67 (s, 1H), 8.61 (d,  $J = 5.2$  Hz, 1H), 8.51 (d,  $J = 1.8$  Hz, 1H), 8.33 (d,  $J = 8.7$  Hz,  
47  
48 1H), 8.22 (dd,  $J = 8.7, 2.0$  Hz, 1H), 7.56 (dd,  $J = 5.2, 1.6$  Hz, 1H), 7.53 (s, 1H), 7.15  
49  
50  
51  
52  
53  
54  
55  
56  
57  
58  
59  
60

(m, 4H), 6.96 (q,  $J = 6.7$  Hz, 1H), 2.63 (s, 3H), 2.21 (d,  $J = 7.7$  Hz, 6H). ESI-MS  $m/z$  380.2  $[M + H]^+$ .

#### 4.1.36.

**(S)-(-)-1-(1-(4-Chlorophenyl)ethyl)-8-(2-methylpyridin-4-yl)-1H-[1,2,3]triazolo[4,5-c]quinolone (9k).** The title compound was prepared from **8k** (50 mg, 129  $\mu\text{mol}$ ) and **29** (18 mg, 129  $\mu\text{mol}$ ) according to the procedure described for compound **1** in 87% yield as a white powder.  $[\alpha]_{\text{D}}^{25} = -277.65$  ( $c = 0.089$ ,  $\text{CH}_3\text{Cl}$ ).  $^1\text{H}$  NMR (400 MHz,  $\text{DMSO-}d_6$ )  $\delta$  9.67 (s, 1H), 8.62 (d,  $J = 5.2$  Hz, 1H), 8.48 (s, 1H), 8.34 (d,  $J = 8.7$  Hz, 1H), 8.23 (d,  $J = 8.7$  Hz, 1H), 7.57 (d,  $J = 5.2$  Hz, 1H), 7.52 (s, 1H), 7.44 (d,  $J = 8.5$  Hz, 2H), 7.29 (d,  $J = 8.5$  Hz, 2H), 7.04 (q,  $J = 6.7$  Hz, 1H), 2.63 (s, 3H), 2.22 (d,  $J = 6.8$  Hz, 3H).  $^{13}\text{C}$  NMR (101 MHz,  $\text{DMSO-}d_6$ )  $\delta$  158.79, 149.72, 145.96, 145.57, 145.11, 140.92, 140.23, 136.43, 132.72, 132.62, 130.97, 129.18, 128.19, 127.65, 121.20, 120.88, 118.86, 115.14, 59.61, 24.20, 22.87. ESI-MS  $m/z$  400.1  $[M + H]^+$ .

#### 4.1.37.

**(S)-1-(1-(4-Fluorophenyl)ethyl)-8-phenyl-1H-[1,2,3]triazolo[4,5-c]quinolone (10).** The title compound was prepared from **8e** (50 mg, 135  $\mu\text{mol}$ ) and commercially available phenylboronic acid (17 mg, 135  $\mu\text{mol}$ ) according to the procedure described for compound **1** in 94% yield as a white powder.  $^1\text{H}$  NMR (400 MHz,  $\text{DMSO-}d_6$ )  $\delta$  9.62 (s, 1H), 8.45 (d,  $J = 1.8$  Hz, 1H), 8.30 (d,  $J = 8.7$  Hz, 1H), 8.15 (dd,  $J = 8.7$ , 2.0 Hz, 1H), 7.73 (d,  $J = 7.2$  Hz, 2H), 7.58 (t,  $J = 8.0$  Hz, 2H), 7.52 – 7.44 (m, 1H), 7.36 – 7.26 (m, 2H), 7.26 – 7.17 (m, 2H), 7.02 (q,  $J = 6.7$  Hz, 1H), 2.20 (d,  $J = 6.8$  Hz, 3H).  $^{13}\text{C}$  NMR (101 MHz,  $\text{DMSO-}d_6$ )  $\delta$  163.27, 160.84, 145.28, 144.83, 141.36, 139.33,

1  
2  
3  
4 138.01, 133.17, 131.22, 129.65, 128.95, 128.69, 128.46, 128.38, 127.78, 121.10,  
5  
6 116.58, 116.37, 115.70, 60.13, 23.56. ESI-MS  $m/z$  369.1  $[M + H]^+$ .  
7

#### 8 9 4.1.38.

10  
11 **(S)-1-(1-(4-Fluorophenyl)ethyl)-8-(6-(4-methylpiperazin-1-yl)pyridin-3-yl)-1H-[1,**  
12  
13 **2,3]triazolo[4,5-*c*]quinolone (11).** The title compound was prepared from **8e** (50 mg,  
14  
15 135  $\mu\text{mol}$ ) and commercially available  
16  
17 (6-(4-methylpiperazin-1-yl)pyridin-3-yl)boronic acid (41 mg, 135  $\mu\text{mol}$ ) using the  
18  
19 procedure described for compound **1** in 72% yield as a pale-yellow powder.  $^1\text{H}$  NMR  
20  
21 (400 MHz,  $\text{DMSO-}d_6$ )  $\delta$  9.56 (s, 1H), 8.59 (d,  $J = 2.5$  Hz, 1H), 8.41 (d,  $J = 1.7$  Hz,  
22  
23 1H), 8.25 (d,  $J = 8.7$  Hz, 1H), 8.12 (dd,  $J = 8.7, 1.8$  Hz, 1H), 7.93 (dd,  $J = 8.9, 2.6$  Hz,  
24  
25 1H), 7.30 (dd,  $J = 8.7, 5.4$  Hz, 2H), 7.19 (t,  $J = 8.8$  Hz, 2H), 7.05 (t,  $J = 6.8$  Hz, 1H),  
26  
27 7.02 (t,  $J = 4.0$  Hz, 1H), 3.61 (d,  $J = 4.7$  Hz, 4H), 2.46 (s, 4H), 2.26 (s, 3H), 2.20 (d,  $J$   
28  
29 = 6.4 Hz, 3H). ESI-MS  $m/z$  468.2  $[M + H]^+$ .  
30  
31  
32  
33  
34  
35

#### 36 37 4.1.39.

38  
39 **(S)-1-(1-(4-Fluorophenyl)ethyl)-8-(pyridin-4-yl)-1H-[1,2,3]triazolo[4,5-*c*]quinolon**  
40  
41 **e (12).** The title compound was prepared from **8e** (50 mg, 135  $\mu\text{mol}$ ) and  
42  
43 commercially available pyridin-4-ylboronic acid (17 mg, 135  $\mu\text{mol}$ ) using the  
44  
45 procedure described for compound **1** in 93% yield as a white powder.  $^1\text{H}$  NMR (400  
46  
47 MHz,  $\text{CDCl}_3$ )  $\delta$  9.68 (s, 1H), 8.77 (d,  $J = 5.1$  Hz, 2H), 8.59 (s, 1H), 8.35 (d,  $J = 8.6$   
48  
49 Hz, 1H), 8.26 (d,  $J = 8.6$  Hz, 1H), 7.80 (d,  $J = 5.1$  Hz, 2H), 7.38 – 7.28 (m, 1H), 7.21  
50  
51 (t,  $J = 8.6$  Hz, 2H), 7.07 (q,  $J = 6.4$  Hz, 1H), 2.22 (d,  $J = 6.6$  Hz, 3H).  $^{13}\text{C}$  NMR (101  
52  
53 MHz,  $\text{DMSO-}d_6$ )  $\delta$  163.27, 160.84, 150.91, 146.22, 146.15, 145.65, 141.39, 137.90,  
54  
55  
56  
57  
58  
59  
60

1  
2  
3  
4 136.67, 132.87, 131.54, 128.64, 128.51, 128.43, 122.20, 121.81, 116.62, 116.40,  
5  
6 115.70, 60.08, 23.53. ESI-MS  $m/z$  370.1  $[M + H]^+$ .  
7

8  
9 **4.1.40.**

10  
11 **(S)-1-(1-(4-Fluorophenyl)ethyl)-8-(2-methoxypyridin-4-yl)-1H-[1,2,3]triazolo[4,5-**  
12  
13 **c]quinolone (13).** The title compound was prepared from **8e** (50 mg, 135  $\mu\text{mol}$ ) and  
14  
15 commercially available (2-methoxypyridin-4-yl)boronic acid (21 mg, 135  $\mu\text{mol}$ ) using  
16  
17 the procedure described for compound **1** in 90% yield as an off-white powder.  $^1\text{H}$   
18  
19 NMR (400 MHz,  $\text{DMSO-}d_6$ )  $\delta$  9.67 (s, 1H), 8.54 (s, 1H), 8.43 - 8.26 (m, 2H), 8.25 -  
20  
21 8.14 (m, 1H), 7.43 - 7.27 (m, 3H), 7.27 - 7.12 (m, 3H), 7.07 (d,  $J = 6.2$  Hz, 1H), 3.97  
22  
23 (s, 3H), 2.22 (d,  $J = 6.6$  Hz, 3H).  $^{13}\text{C}$  NMR (101 MHz,  $\text{DMSO-}d_6$ )  $\delta$  165.03, 163.24,  
24  
25 160.81, 149.45, 148.18, 146.10, 145.68, 141.37, 137.89, 136.66, 133.16, 131.42,  
26  
27 128.74, 128.47, 128.38, 121.78, 116.59, 116.37, 115.92, 115.62, 108.76, 60.04, 53.88,  
28  
29 23.49. ESI-MS  $m/z$  400.2  $[M + H]^+$ .  
30  
31  
32  
33  
34  
35

36  
37 **4.1.41.**

38  
39 **(S)-1-(1-(4-Fluorophenyl)ethyl)-8-(4-methoxyphenyl)-1H-[1,2,3]triazolo[4,5-c]qui**  
40  
41 **nolone (14).** The title compound was prepared from **8e** (50 mg, 135  $\mu\text{mol}$ ) and  
42  
43 commercially available (4-methoxyphenyl)boronic acid (21 mg, 135  $\mu\text{mol}$ ) using the  
44  
45 procedure described for compound **1** in 89% yield as an off-white powder.  $^1\text{H}$  NMR  
46  
47 (400 MHz,  $\text{CDCl}_3$ )  $\delta$  9.58 (s, 1H), 8.38 (s, 1H), 8.25 (d,  $J = 8.6$  Hz, 1H), 8.11 (d,  $J =$   
48  
49 8.6 Hz, 1H), 7.68 (d,  $J = 8.4$  Hz, 2H), 7.34 - 7.27 (m, 2H), 7.22 (t,  $J = 8.6$  Hz, 2H),  
50  
51 7.14 (d,  $J = 8.4$  Hz, 2H), 7.00 (q,  $J = 6.4$  Hz, 1H), 3.86 (s, 3H), 2.20 (d,  $J = 6.6$  Hz,  
52  
53 3H).  $^{13}\text{C}$  NMR (101 MHz,  $\text{DMSO-}d_6$ )  $\delta$  163.26, 160.83, 160.03, 144.85, 144.44,  
54  
55  
56  
57  
58  
59  
60

1  
2  
3  
4 141.36, 139.40, 138.06, 133.11, 131.57, 131.12, 128.94, 128.58, 128.44, 128.36,  
5  
6 120.18, 116.61, 116.40, 115.73, 115.11, 60.12, 55.80, 23.59. ESI-MS  $m/z$  399.1 [M +  
7  
8 H]<sup>+</sup>.  
9

#### 10 11 4.1.42.

12  
13 **(S)-4-(1-(1-(4-Fluorophenyl)ethyl)-1H-[1,2,3]triazolo[4,5-c]quinolin-8-yl)benzami**  
14  
15 **de (15).** The title compound was prepared from **8e** (48 mg, 129  $\mu\text{mol}$ ) and  
16  
17 commercially available (4-carbamoylphenyl)boronic acid (21 mg, 129  $\mu\text{mol}$ ) using  
18  
19 the procedure described for compound **1** in 88% yield as a yellow powder. <sup>1</sup>H NMR  
20  
21 (400 MHz, DMSO-*d*<sub>6</sub>)  $\delta$  9.64 (s, 1H), 8.50 (d, *J* = 1.7 Hz, 1H), 8.32 (d, *J* = 8.7 Hz,  
22  
23 1H), 8.21 (dd, *J* = 8.7, 1.9 Hz, 1H), 8.12 (s, 1H), 8.09 (d, *J* = 8.4 Hz, 2H), 7.81 (d, *J* =  
24  
25 8.4 Hz, 2H), 7.49 (s, 1H), 7.36 – 7.28 (m, 2H), 7.22 (t, *J* = 8.8 Hz, 2H), 7.04 (q, *J* =  
26  
27 6.7 Hz, 1H), 2.22 (d, *J* = 6.7 Hz, 3H). <sup>13</sup>C NMR (101 MHz, DMSO-*d*<sub>6</sub>)  $\delta$  167.89,  
28  
29 163.27, 160.84, 145.58, 145.06, 141.87, 141.39, 138.75, 137.99, 134.21, 133.18,  
30  
31 131.29, 128.99, 128.81, 128.44, 128.36, 127.58, 121.47, 116.61, 116.39, 115.69,  
32  
33 60.13, 23.60. ESI-MS  $m/z$  412.2 [M + H]<sup>+</sup>.  
34  
35  
36  
37  
38  
39  
40

#### 41 4.1.43.

42  
43 **(S)-4-(1-(1-(4-Fluorophenyl)ethyl)-1H-[1,2,3]triazolo[4,5-c]quinolin-8-yl)morphol**  
44  
45 **ine (16).** Compound **8e** (50 mg, 135  $\mu\text{mol}$ , 1 equiv), morpholine (117 mg, 1.35 mmol,  
46  
47 10 equiv), Pd<sub>2</sub>(dba)<sub>3</sub> (12 mg, 13.5  $\mu\text{mol}$ , 0.1 equiv), X-Phos (13 mg, 27  $\mu\text{mol}$ , 0.2  
48  
49 equiv) and K<sub>2</sub>CO<sub>3</sub> (56 mg, 405  $\mu\text{mol}$ , 3 equiv) were suspended in *t*-BuOH. Under a  
50  
51 nitrogen atmosphere, the mixture was stirred at 100 °C overnight. The solvent was  
52  
53 evaporated to dryness under reduced pressure to give the crude product, which was  
54  
55  
56  
57  
58  
59  
60

1  
2  
3  
4 purified by flash column chromatography to yield the desired product as white  
5  
6 powder (42.3 mg, 83% yield).  $^1\text{H}$  NMR (400 MHz,  $\text{DMSO-}d_6$ )  $\delta$  9.33 (s, 1H), 8.02 (d,  
7  
8  $J = 9.2$  Hz, 1H), 7.56 (d,  $J = 9.2$  Hz, 1H), 7.41 – 7.31 (m, 3H), 7.27 (t,  $J = 7.2$  Hz, 1H),  
9  
10 7.17 (d,  $J = 7.6$  Hz, 2H), 6.83 (q,  $J = 6.4$  Hz, 1H), 3.78 (t,  $J = 4.6$  Hz, 4H), 3.31 – 3.21  
11  
12 (m, 2H), 3.17 – 3.06 (m, 2H), 2.18 (d,  $J = 6.7$  Hz, 3H).  $^{13}\text{C}$  NMR (101 MHz,  
13  
14  $\text{DMSO-}d_6$ )  $\delta$  163.25, 160.82, 150.13, 141.47, 141.33, 139.63, 138.31, 132.60, 131.27,  
15  
16 128.24, 128.15, 119.83, 116.58, 116.36, 104.95, 66.37, 60.03, 48.41, 23.67. ESI-MS  
17  
18 m/z: 378.1  $[\text{M} + \text{H}]^+$ .  
19  
20  
21  
22

#### 23 24 4.1.44.

25  
26 **(S)-8-(4-Fluoro-3-methylphenyl)-1-(1-(4-fluorophenyl)ethyl)-1*H*-[1,2,3]triazolo[4,**  
27  
28 **5-*c*]quinolone (17).** The title compound was prepared from **8e** (50 mg, 135  $\mu\text{mol}$ ) and  
29  
30 commercially available (4-fluoro-3-methylphenyl)boronic acid (21 mg, 135  $\mu\text{mol}$ )  
31  
32 using the procedure described for compound **1** in 92% yield as a white powder.  $^1\text{H}$   
33  
34 NMR (400 MHz,  $\text{CDCl}_3$ )  $\delta$  9.59 (s, 1H), 8.34 (d,  $J = 8.6$  Hz, 1H), 8.10 (d,  $J = 1.8$  Hz,  
35  
36 1H), 7.92 (dd,  $J = 8.6, 2.0$  Hz, 1H), 7.26 – 7.18 (m, 3H), 7.14 (t,  $J = 8.8$  Hz, 1H), 7.11  
37  
38 – 7.04 (m, 2H), 6.46 (q,  $J = 6.9$  Hz, 1H), 2.40 (d,  $J = 1.8$  Hz, 3H), 2.32 (d,  $J = 7.0$  Hz,  
39  
40 3H).  $^{13}\text{C}$  NMR (101 MHz,  $\text{DMSO-}d_6$ )  $\delta$  163.24, 162.59, 160.81, 160.15, 145.24,  
41  
42 144.71, 141.38, 138.75, 138.06, 138.03, 135.45, 135.42, 133.15, 131.15, 130.99,  
43  
44 130.93, 128.82, 128.36, 128.28, 127.09, 127.01, 125.57, 125.39, 120.90, 116.62,  
45  
46 116.40, 116.23, 116.01, 115.64, 60.12, 23.61, 14.81, 14.78. ESI-MS m/z 401.0  $[\text{M} +$   
47  
48  $\text{H}]^+$ .  
49  
50  
51  
52  
53  
54

#### 55 56 4.1.45.

1  
2  
3  
4 **(S)-4-(1-(1-(4-Fluorophenyl)ethyl)-1H-[1,2,3]triazolo[4,5-c]quinolin-8-yl)benzonit**  
5  
6 **rile (18)**. The title compound was prepared from **8e** (50 mg, 135  $\mu\text{mol}$ ) and  
7  
8 commercially available (4-cyanophenyl)boronic acid (20 mg, 135  $\mu\text{mol}$ ) using the  
9  
10 procedure described for compound **1** in 91% yield as an off-white powder.  $^1\text{H}$  NMR  
11  
12 (400 MHz,  $\text{DMSO-}d_6$ )  $\delta$  9.66 (s, 1H), 8.53 (d,  $J = 1.8$  Hz, 1H), 8.34 (d,  $J = 8.7$  Hz,  
13  
14 1H), 8.22 (dd,  $J = 8.7, 2.0$  Hz, 1H), 8.07 (d,  $J = 8.5$  Hz, 2H), 7.96 (d,  $J = 8.5$  Hz, 2H),  
15  
16 7.35 – 7.27 (m, 2H), 7.21 (t,  $J = 9.2$  Hz, 2H), 7.04 (q,  $J = 6.7$  Hz, 1H), 2.20 (d,  $J = 6.8$   
17  
18 Hz, 3H). ESI-MS  $m/z$  394.1  $[\text{M} + \text{H}]^+$ .

#### 23 24 4.1.46.

25  
26 **(S)-1-(1-(4-Fluorophenyl)ethyl)-8-(pyridin-3-yl)-1H-[1,2,3]triazolo[4,5-c]quinolon**  
27  
28 **e (19)**. The title compound was prepared from **8e** (50 mg, 135  $\mu\text{mol}$ ) and  
29  
30 commercially available pyridin-3-ylboronic acid (17 mg, 135  $\mu\text{mol}$ ) using the  
31  
32 procedure described for compound **1** in 90% yield as a white powder.  $^1\text{H}$  NMR (400  
33  
34 MHz,  $\text{DMSO-}d_6$ )  $\delta$  9.65 (s, 1H), 8.99 (d,  $J = 2.4$  Hz, 1H), 8.68 (dd,  $J = 4.8, 1.5$  Hz,  
35  
36 1H), 8.55 (d,  $J = 1.6$  Hz, 1H), 8.34 (d,  $J = 8.6$  Hz, 1H), 8.25 – 8.12 (m, 2H), 7.62 (dd,  
37  
38  $J = 7.9, 4.8$  Hz, 1H), 7.36 – 7.27 (m, 2H), 7.24 – 7.14 (m, 2H), 7.08 (q,  $J = 6.7$  Hz,  
39  
40 1H), 2.21 (d,  $J = 6.8$  Hz, 3H).  $^{13}\text{C}$  NMR (101 MHz,  $\text{DMSO-}d_6$ )  $\delta$  162.74, 160.31,  
41  
42 149.13, 148.16, 145.21, 144.59, 140.84, 137.44, 137.41, 136.20, 134.71, 134.35,  
43  
44 132.59, 130.98, 128.49, 127.99, 127.91, 123.99, 120.87, 116.03, 115.82, 115.25,  
45  
46 59.46, 22.98. ESI-MS  $m/z$  370.1  $[\text{M} + \text{H}]^+$ .

#### 53 54 4.1.47.

55  
56 **(S)-1-(1-(4-Fluorophenyl)ethyl)-8-(1-methyl-1H-pyrazol-4-yl)-1H-[1,2,3]triazolo[**  
57  
58  
59  
60

1  
2  
3  
4 **4,5-*c*]quinolone (20).** The title compound was prepared from **8e** (100 mg, 269  $\mu\text{mol}$ )  
5  
6 and commercially available (1-methyl-1*H*-pyrazol-4-yl)boronic acid (56 mg, 269  
7  
8  $\mu\text{mol}$ ) using the procedure described for compound **1** in 83% yield as an off-white  
9  
10 powder.  $^1\text{H}$  NMR (400 MHz,  $\text{DMSO-}d_6$ )  $\delta$  9.51 (s, 1H), 8.35 (s, 2H), 8.18 (d,  $J = 8.7$   
11  
12 Hz, 1H), 8.08 (s, 1H), 8.05 (d,  $J = 8.7$  Hz, 1H), 7.34 (dd,  $J = 8.7, 5.4$  Hz, 2H), 7.18 (t,  
13  
14  $J = 8.8$  Hz, 2H), 7.01 (q,  $J = 6.7$  Hz, 1H), 3.95 (s, 3H), 2.22 (d,  $J = 6.8$  Hz, 3H).  $^{13}\text{C}$   
15  
16 NMR (101 MHz,  $\text{DMSO-}d_6$ )  $\delta$  163.20, 160.77, 144.19, 144.00, 141.34, 138.01,  
17  
18 137.15, 132.84, 132.55, 131.21, 129.26, 128.45, 128.37, 127.59, 121.37, 117.88,  
19  
20 116.51, 116.30, 115.93, 59.92, 39.34, 23.53. ESI-MS  $m/z$  373.2  $[\text{M} + \text{H}]^+$ .

#### 21 22 23 24 25 26 **4.1.48.**

27  
28 **(*S*)-1-(5-(1-(1-(4-Fluorophenyl)ethyl)-1*H*-[1,2,3]triazolo[4,5-*c*]quinolin-8-yl)thiop**  
29  
30 **hen-2-yl)ethan-1-one (21).** The title compound was prepared from **8e** (50 mg, 135  
31  
32  $\mu\text{mol}$ ) and commercially available (5-acetylthiophen-2-yl)boronic acid (23 mg, 135  
33  
34  $\mu\text{mol}$ ) using the procedure described for compound **1** in 74% yield as an off-white  
35  
36 powder.  $^1\text{H}$  NMR (400 MHz,  $\text{DMSO-}d_6$ )  $\delta$  9.64 (s, 1H), 8.50 (d,  $J = 1.8$  Hz, 1H), 8.28  
37  
38 (d,  $J = 8.7$  Hz, 1H), 8.22 (dd,  $J = 8.7, 2.0$  Hz, 1H), 8.06 (d,  $J = 4.0$  Hz, 1H), 7.85 (d,  $J$   
39  
40 = 4.0 Hz, 1H), 7.37 – 7.29 (m, 2H), 7.21 – 7.13 (m, 2H), 7.02 (q,  $J = 6.6$  Hz, 1H),  
41  
42 2.61 (s, 3H), 2.22 (d,  $J = 6.8$  Hz, 3H).  $^{13}\text{C}$  NMR (101 MHz,  $\text{DMSO-}d_6$ )  $\delta$  191.17,  
43  
44 163.22, 160.79, 150.09, 145.86, 145.39, 144.44, 141.49, 137.75, 137.72, 135.61,  
45  
46 132.95, 132.15, 131.61, 128.43, 128.35, 127.84, 127.06, 120.27, 116.59, 116.38,  
47  
48 115.78, 60.18, 26.94, 23.54. ESI-MS  $m/z$  417.1  $[\text{M} + \text{H}]^+$ .

#### 49 50 51 52 53 54 55 56 **4.1.49.**



1  
2  
3  
4 **(S)-4-(1-(1-(4-Fluorophenyl)ethyl)-1H-[1,2,3]triazolo[4,5-c]quinolin-8-yl)-3,5-dim**  
5 **ethylisoxazole (22).** The title compound was prepared from **8e** (50 mg, 135  $\mu\text{mol}$ ) and  
6 commercially available (3,5-dimethylisoxazol-4-yl)boronic acid (19 mg, 135  $\mu\text{mol}$ )  
7 using the procedure described for compound **1** in 85% yield as an off-white powder.  
8  
9  
10  
11  
12  
13  $^1\text{H}$  NMR (400 MHz, DMSO- $d_6$ )  $\delta$  9.66 (s, 1H), 8.33 (d,  $J$  = 8.6 Hz, 1H), 8.28 (d,  $J$  =  
14 1.6 Hz, 1H), 7.87 (dd,  $J$  = 8.6, 1.7 Hz, 1H), 7.26 – 7.14 (m, 4H), 6.93 (q,  $J$  = 6.6 Hz,  
15 1H), 2.31 (s, 3H), 2.16 (d,  $J$  = 6.8 Hz, 3H), 2.14 (s, 3H).  $^{13}\text{C}$  NMR (101 MHz,  
16 DMSO- $d_6$ )  $\delta$  166.38, 163.25, 160.82, 158.71, 145.66, 144.68, 141.16, 137.54, 132.99,  
17 131.23, 131.14, 129.97, 128.48, 128.40, 123.37, 116.41, 116.19, 115.93, 115.75, 59.78,  
18 23.42, 11.68, 10.72. ESI-MS  $m/z$  388.2  $[\text{M} + \text{H}]^+$ .  
19  
20  
21  
22  
23  
24  
25  
26  
27  
28

#### 29 4.1.50.

30  
31 **(S)-8-(Benzo[*d*][1,3]dioxol-5-yl)-1-(1-(4-fluorophenyl)ethyl)-1H-[1,2,3]triazolo[4,5**  
32 **-c]quinolone (23).** The title compound was prepared from **8e** (50 mg, 135  $\mu\text{mol}$ ) and  
33 commercially available benzo[*d*][1,3]dioxol-5-yl boronic acid (22 mg, 135  $\mu\text{mol}$ )  
34 using the procedure described for compound **1** in 83% yield as an off-white powder.  
35  
36  
37  
38  
39  
40  
41  $^1\text{H}$  NMR (400 MHz, DMSO- $d_6$ )  $\delta$  9.59 (s, 1H), 8.36 (d,  $J$  = 1.9 Hz, 1H), 8.25 (d,  $J$  =  
42 8.7 Hz, 1H), 8.09 (dd,  $J$  = 8.7, 2.0 Hz, 1H), 7.33 (d,  $J$  = 1.8 Hz, 1H), 7.32 – 7.26 (m,  
43 2H), 7.24 – 7.15 (m, 3H), 7.12 (d,  $J$  = 8.1 Hz, 1H), 7.02 (q,  $J$  = 6.7 Hz, 1H), 6.14 (d,  $J$   
44 = 1.7 Hz, 2H), 2.20 (d,  $J$  = 6.8 Hz, 3H).  $^{13}\text{C}$  NMR (101 MHz, DMSO- $d_6$ )  $\delta$  163.23,  
45 160.80, 148.72, 148.02, 144.99, 144.57, 141.34, 139.46, 138.03, 138.00, 133.49,  
46 133.10, 131.08, 128.83, 128.42, 128.34, 121.67, 120.45, 116.56, 116.34, 115.66,  
47 109.35, 108.03, 101.90, 60.05, 23.54. ESI-MS  $m/z$  413.1  $[\text{M} + \text{H}]^+$ .  
48  
49  
50  
51  
52  
53  
54  
55  
56  
57  
58  
59  
60

**4.1.51.**

**(S)-8-(Benzofuran-5-yl)-1-(1-(4-fluorophenyl)ethyl)-1H-[1,2,3]triazolo[4,5-c]quinoline (24).** The title compound was prepared from **8e** (100 mg, 269  $\mu\text{mol}$ ) and commercially available benzofuran-5-ylboronic acid (66 mg, 269  $\mu\text{mol}$ ) using the procedure described for compound **1** in 86% yield as an off-white powder.  $^1\text{H}$  NMR (400 MHz,  $\text{DMSO-}d_6$ )  $\delta$  9.61 (s, 1H), 8.46 (d,  $J = 1.8$  Hz, 1H), 8.30 (d,  $J = 8.7$  Hz, 1H), 8.18 (dd,  $J = 8.7, 2.0$  Hz, 1H), 8.12 (d,  $J = 2.2$  Hz, 1H), 7.93 (d,  $J = 1.7$  Hz, 1H), 7.80 (d,  $J = 8.6$  Hz, 1H), 7.66 (dd,  $J = 8.6, 1.9$  Hz, 1H), 7.36 – 7.28 (m, 2H), 7.28 – 7.20 (m, 2H), 7.13 (dd,  $J = 2.2, 0.9$  Hz, 1H), 7.02 (q,  $J = 6.7$  Hz, 1H), 2.21 (d,  $J = 6.8$  Hz, 3H).  $^{13}\text{C}$  NMR (101 MHz,  $\text{DMSO-}d_6$ )  $\delta$  163.30, 160.87, 154.82, 147.55, 145.08, 144.77, 144.61, 141.39, 140.15, 138.06, 134.64, 133.16, 131.15, 129.28, 128.57, 128.46, 128.38, 124.51, 121.24, 120.60, 116.65, 116.43, 115.71, 112.36, 107.56, 60.16, 23.57. ESI-MS  $m/z$  409.0  $[\text{M} + \text{H}]^+$ .

**4.1.52.**

**(S)-(-)-5-(1-(1-(4-Fluorophenyl)ethyl)-1H-[1,2,3]triazolo[4,5-c]quinolin-8-yl)benzo[d]oxazole (25).** The title compound was prepared from **8e** (200 mg, 539  $\mu\text{mol}$ ) and self-prepared compound **28** (132 mg, 539  $\mu\text{mol}$ ) using the procedure described for compound **1** in 86% yield as a white powder, 99.1% HPLC purity.  $[\alpha]_D^{25} = -238.32$  (c = 0.107,  $\text{CH}_3\text{Cl}$ , ee 100%).  $^1\text{H}$  NMR (400 MHz,  $\text{DMSO-}d_6$ )  $\delta$  9.63 (s, 1H), 8.87 (s, 1H), 8.52 (d,  $J = 1.4$  Hz, 1H), 8.32 (d,  $J = 8.7$  Hz, 1H), 8.24 (dd,  $J = 8.7, 1.7$  Hz, 1H), 8.18 (d,  $J = 1.0$  Hz, 1H), 8.00 (d,  $J = 8.3$  Hz, 1H), 7.78 (dd,  $J = 8.3, 1.5$  Hz, 1H), 7.32 (dd,  $J = 8.6, 5.4$  Hz, 2H), 7.20 (t,  $J = 8.8$  Hz, 2H), 7.07 (q,  $J = 6.6$  Hz, 1H), 2.22 (d,  $J$

1  
2  
3  
4 = 6.7 Hz, 3H).  $^{13}\text{C}$  NMR (101 MHz, DMSO- $d_6$ )  $\delta$  163.26, 160.83, 155.66, 150.72,  
5  
6 145.46, 144.89, 141.39, 140.22, 139.24, 138.01, 137.36, 133.16, 131.29, 129.39,  
7  
8 128.48, 128.40, 124.84, 121.56, 121.02, 116.60, 116.39, 115.72, 110.50, 60.07, 23.56.  
9  
10  $^{19}\text{F}$  NMR (376 MHz, TFA- $d$ )  $\delta$  -110.76. ESI-MS  $m/z$  410.1  $[\text{M} + \text{H}]^+$ . HRMS  $m/z$   
11  
12 (ESI) calcd for  $\text{C}_{24}\text{H}_{17}\text{FN}_5\text{O}$   $[\text{M} + \text{H}]^+$  410.1412; found, 410.1410. HPLC purity  
13  
14 analysis (mobile phase:  $\text{H}_2\text{O}/\text{MeOH} = 25/75$ , flow rate = 1.0 mL/min,  $\lambda = 255.9$  nm,  
15  
16  $t_{\text{R}} = 7.05$  min). Chiral HPLC analysis (mobile phase: 2-propanol/n-hexane = 30/70,  
17  
18 flow rate = 1.0 mL/min,  $\lambda = 255.9$  nm,  $t_{\text{R}} = 40.50$  min).  
19  
20  
21  
22  
23

24 **4.1.53. 5-Bromobenzo[d]oxazole (27).** 2-Amino-4-bromophenol (**26**, 2 g, 10.64  
25  
26 mmol) was added to triethyl orthoformate (30 mL) under a nitrogen atmosphere. The  
27  
28 resulting mixture was refluxed for 8 h and monitored by TLC. After cooling to rt,  
29  
30 triethyl orthoformate was removed under reduced pressure at 80 °C, and the residue  
31  
32 was purified by column chromatography to yield the desired products as a white solid  
33  
34 (1.89 g, 90% yield).  $^1\text{H}$  NMR (400 MHz, DMSO- $d_6$ )  $\delta$  8.82 (s, 1H), 8.07 (d,  $J = 1.9$   
35  
36 Hz, 1H), 7.79 (d,  $J = 8.7$  Hz, 1H), 7.62 (dd,  $J = 8.7, 2.0$  Hz, 1H).  
37  
38  
39  
40

41 **4.1.54. 5-(4,4,5,5-Tetramethyl-1,3,2-dioxaborolan-2-yl)benzo[d]oxazole (28).**  
42  
43 To a suspension of **27** (1 g, 5.05 mmol, 1 equiv), bis(pinacolato)diboron (1.54 g, 6.06  
44  
45 mmol, 1.2 equiv) and potassium acetate (1.49 g, 15.15 mmol, 3 equiv) in 1,4-dioxane,  
46  
47 Pd(dppf) $\text{Cl}_2$  (184.76 mg, 0.25 mmol, 0.05 equiv) was added, and the mixture was  
48  
49 stirred at 100 °C under a nitrogen atmosphere for 8 h. After cooling to rt, the solvent  
50  
51 was evaporated to dryness under reduced pressure to obtain the crude product, which  
52  
53 was purified by flash column chromatography to yield the desired product as an  
54  
55  
56  
57  
58  
59  
60

1  
2  
3  
4 off-white powder (1.03 g, 83% yield).  $^1\text{H}$  NMR (400 MHz,  $\text{DMSO-}d_6$ )  $\delta$  8.80 (s, 1H),  
5  
6 8.05 (s, 1H), 7.79 (d,  $J = 8.2$  Hz, 1H), 7.76 (d,  $J = 8.2$  Hz, 1H), 1.33 (s, 12H).  $^{13}\text{C}$   
7  
8 NMR (101 MHz,  $\text{DMSO-}d_6$ )  $\delta$  154.87, 152.05, 140.05, 132.20, 126.71, 125.29,  
9  
10 111.42, 84.33, 25.13. ESI-MS  $m/z$  246.1  $[\text{M} + \text{H}]^+$ .  
11  
12

## 13 14 **4.2. Pharmacological Experiments**

15  
16 **4.2.1. *In Vitro* Kinase Activity Assays.** CLK1 and DYRK1A kinase assays were  
17  
18 conducted using the KinaseProfiler service of Eurofins Pharma Discovery Services  
19  
20 UK Limited according to the protocols described below (for details on more kinases,  
21  
22 see <http://www.eurofins.com/pharmadiscovery>). The concentration of ATP in each  
23  
24 assay was 10  $\mu\text{M}$ .  
25  
26  
27

28  
29 CLK1 (h) was incubated with 8 mM MOPS, pH 7.0; 0.2 mM EDTA; 1 mM  
30  
31 sodium orthovanadate; 5 mM sodium  $\beta$ -glycerophosphate; 200  $\mu\text{M}$   
32  
33 ERMRPRKRQGSVRRRV; 10 mM magnesium acetate; and  $[\gamma\text{-}^{33}\text{P}]\text{-ATP}$  (specific  
34  
35 activity and concentration as required). The reaction was initiated by addition of the  
36  
37 Mg/ATP mixture. After incubation for 40 min at rt, the reaction was stopped by the  
38  
39 addition of phosphoric acid at a concentration of 0.5%. A total of 10  $\mu\text{L}$  of the  
40  
41 reaction was then spotted onto a P30 filtermat, followed by washing four times for 4  
42  
43 min in 0.425% phosphoric acid and once in methanol prior to drying and scintillation  
44  
45 counting.  
46  
47  
48  
49

50  
51 DYRK1A (h) was incubated with 8 mM MOPS, pH 7.0; 0.2 mM EDTA; 50  $\mu\text{M}$   
52  
53 RRRFRPASPLRGPPK; 10 mM magnesium acetate; and  $[\gamma\text{-}^{33}\text{P}]\text{-ATP}$  (specific  
54  
55 activity and concentration as required). The reaction was initiated by addition of the  
56  
57  
58  
59  
60

1  
2  
3  
4 Mg/ATP mixture. After incubation for 40 min at rt, the reaction was stopped by the  
5  
6 addition of phosphoric acid at a concentration of 0.5%. A total of 10  $\mu$ L of the  
7  
8 reaction was then spotted onto a P30 filtermat, followed by washing four times for 4  
9  
10 min in 0.425% phosphoric acid and once in methanol prior to drying and scintillation  
11  
12 counting.  
13  
14  
15

16 **4.2.2. Cell Culturing and Infection with Ad-mRFP-GFP-LC3.** BNL CL.2 and  
17  
18 SKOV-3 cells were maintained in Dulbecco's modified Eagle's medium and  
19  
20 RPMI1640 media, respectively, both of which were supplemented with 10% fetal  
21  
22 bovine serum. For adenovirus infection, SKOV-3 cells were cultured with a half  
23  
24 volume of culture media for 4 h that contained Ad-mRFP-GFP-LC3 (adenovirus  
25  
26 coding tandem GFP-mRFP-LC3, Hanbio) and 5  $\mu$ g/mL polybrene. Then, the media  
27  
28 was refreshed with culture media containing compound **25** or DMSO (0.1%). Cells  
29  
30 were grown at 37  $^{\circ}$ C and 5% CO<sub>2</sub> in a humidified incubator.  
31  
32  
33  
34  
35

36 **4.2.3. Immunoblot Assays.** Whole cell lysates were extracted with  
37  
38 radioimmunoprecipitation assay (RIPA) lysis buffer (Beyotime Biotechnology) that  
39  
40 contained phenylmethanesulfonyl fluoride (PMSF, Sigma), protease inhibitor cocktail  
41  
42 (Sigma) and phosphatase inhibitor cocktail (Biotool.com). An equal amount of protein  
43  
44 (10–25  $\mu$ g/lane) was resolved by 12% or 10% sodium dodecyl sulfate polyacrylamide  
45  
46 gel electrophoresis (SDS-PAGE) and transferred to polyvinylidene fluoride (PVDF)  
47  
48 membranes (Millipore). The membranes were blocked with TBS-T blocking buffer (5%  
49  
50 nonfat milk in TBS-T) for 2–3 h at rt and then probed with primary antibodies  
51  
52 overnight at 4  $^{\circ}$ C. After three washes with TBS-T, the membranes were incubated  
53  
54  
55  
56  
57  
58  
59  
60

1  
2  
3  
4 with horseradish peroxidase-conjugated goat anti-mouse or anti-rabbit antibody (Cell  
5  
6 Signaling Technology, 1:5000 dilution) for 1 h at 37 °C. After extensive washing with  
7  
8 TBS-T, the membranes were preserved in TBS, and the immunoblots were visualized  
9  
10 by ECL (Abbkine). Anti-LC3B (NOVUS, NB 600-1384, 1:1000 dilution) and  
11  
12 anti-SQSTM1/p62 (Proteintech, 1:1000 dilution) antibodies were used to detect the  
13  
14 level of autophagy and the degradation of autophagosomes, respectively, while  
15  
16 anti-GAPDH antibodies (Cell Signaling Technology, 1:1000 dilution) were used to  
17  
18 probe GAPDH as a control. Immunoblots were quantified using Adobe Photoshop  
19  
20 software.  
21  
22  
23  
24

25  
26 **4.2.4. Immunofluorescence and Confocal Microscopy.** For  
27  
28 immunofluorescence, BNL CL.2 cells were treated with media containing **25** or  
29  
30 DMSO for 24 h. Then, the cells were washed gently with PBS three times and fixed  
31  
32 with 4% paraformaldehyde solution for 30 min. Fixed cells were washed with PBS  
33  
34 and permeabilized with 0.5% Triton X-100 solution for 20 min. After three washes  
35  
36 with PBS, cells were blocked by PBS blocking buffer (10% bovine albumin in PBS)  
37  
38 for 30 min at rt. Then, the cells were incubated with anti-SR proteins antibody  
39  
40 (mAb1H4G7, Invitrogen, 1:200 dilution) overnight at 4 °C to probe phosphorylated  
41  
42 SR proteins. After three washes with PBS, in the absence of illumination, the cells  
43  
44 were incubated with a secondary antibody (Cy3-conjugated AffiniPure goat  
45  
46 anti-mouse IgG antibody, Proteintech, 1:50 dilution) for 30 min at 37 °C. Then, 0.5  
47  
48 µg/mL 4',6-diamidino-2-phenylindole (DAPI) was used to visualize nuclei. Before  
49  
50 examination, the cells were washed with PBS four times to remove residual DAPI.  
51  
52  
53  
54  
55  
56  
57  
58  
59  
60

1  
2  
3  
4 After treatment with **25** or DMSO, Ad-mRFP-GFP-LC3-infected cells were fixed with  
5  
6 4% paraformaldehyde solution before examination. The cells were viewed with an  
7  
8 upright Leica confocal laser scanning microscope equipped with 40× and 63× oil  
9  
10 immersion lenses.  
11

12  
13 **4.2.5. *In Vivo* Study.** Animal studies were conducted under the approval of the  
14  
15 Experimental Animal Management Committee of Sichuan University. Male C57BL/6  
16  
17 mice were given either saline (n = 3, ip) or APAP (500 mg/kg) (n = 15, ip). To  
18  
19 examine the hepatoprotective effect, mice were injected (ip) with **25** (30 mg/kg), **30**  
20  
21 (30 mg/kg, positive control), rapamycin (30 mg/kg, positive control), or solvent (12.5%  
22  
23 ethanol and 12.5% castor oil, 10 ml/kg), immediately followed by APAP (500 mg/kg)  
24  
25 injection (ip). All mice were sacrificed 6 h later. Liver sections were examined by  
26  
27 H&E staining, and the serum from the blood samples was used for ALT and AST  
28  
29 activity tests.  
30  
31  
32  
33  
34  
35

### 36 **4.3. *CLK1/Inhibitor Co-crystallization and Structure Determination***

37  
38 **4.3.1. Plasmid Construction.** The coding sequence of human CLK1 (residues:  
39  
40 147–483) was cloned into the NdeI and XhoI restriction sites of pET22b (+) vector  
41  
42 with a C-terminal His tag. The recombinant plasmid was successfully verified by  
43  
44 DNA sequencing.  
45  
46  
47

48  
49 **4.3.2. Protein Expression and Purification.** The plasmid was transformed into  
50  
51 *Escherichia coli* BL21 (DE3) competent cells. The transformant was grown at 37 °C  
52  
53 until an OD<sub>600</sub> of 0.8 was reached and induced with 1 mM isopropyl-β-D-  
54  
55 thiogalactoside (IPTG) at 18 °C overnight. The cells were resuspended in lysis buffer  
56  
57  
58  
59  
60

1  
2  
3  
4 (50 mM HEPES (pH 7.5), 500 mM NaCl, 5% glycerol, 50 mM L-glutamic acid, and  
5  
6 50 mM L-arginine), and lysed using a high pressure homogenizer at 4 °C. The  
7  
8 insoluble debris was removed by centrifugation. The lysate was purified from the  
9  
10 supernatants using Ni-NTA column chromatography. The eluted protein was further  
11  
12 purified by size exclusion chromatography using a Superdex<sup>®</sup> 200 Increase 10/300  
13  
14 GL (GE Healthcare) column in lysis buffer. The purified proteins were treated with  
15  
16 lambda phosphatase overnight at 4 °C to remove phosphorylation, and passed through  
17  
18 the Superdex<sup>®</sup> 200 (10/300 GL) column again. The protein peak corresponding to  
19  
20 homogenous protein was collected. The quality of all purified samples was validated  
21  
22 by SDS-PAGE analysis.  
23  
24  
25  
26  
27

28  
29 **4.3.3. Crystallization and Data Collection.** For co-crystallization, CLK1  
30  
31 protein was concentrated to 13 mg/mL and mixed with saturated X solution overnight  
32  
33 in lysis buffer (50 mM HEPES (pH 7.5), 500 mM NaCl, 5% glycerol, 50 mM  
34  
35 L-glutamic acid, and 50 mM L-arginine). The mixture was crystallized by the  
36  
37 sitting-drop vapor diffusion method at 18 °C. Diffractable crystals of the complex  
38  
39 were obtained in a condition consisting of 2% (v/v) PEG 200, 20% (v/v) tacsimate  
40  
41 (pH 7.0), and 0.1 M HEPES (pH 9.0) and cryoprotected in the same precipitate  
42  
43 solution containing 33% (v/v) glycerol. The diffraction data were collected at  
44  
45 beamline BL17U1<sup>41</sup> of Shanghai Synchrotron Radiation Facility (SSRF) using the  
46  
47 synchrotron radiation. Data were then processed and scaled using the programs of  
48  
49 HKL2000.<sup>42</sup>  
50  
51  
52  
53  
54

55  
56 **4.3.4. Structure Determination.** The complex structure was solved by  
57  
58  
59  
60



1  
2  
3  
4 molecular replacement module of PHASER<sup>43</sup> from the CCP4 program suite,<sup>44</sup> and the  
5  
6 CLK1/**25** complex structure was solved with a previously reported CLK1 structure  
7  
8 (PDB ID 2VAG) as the search model. The built structure model was further refined  
9  
10 using REFMAC<sup>45</sup> and Phenix.<sup>46</sup> The atomic model was completed with Coot<sup>47</sup> and  
11  
12 refined with phenix.refine.<sup>46</sup> The program of PROCHECK was used to assess the  
13  
14 stereochemistry of the final model.  
15  
16  
17  
18  
19  
20

## 21 ASSOCIATED CONTENT

### 22 Supporting Information

23  
24 Kinase inhibition profiles of **25** against a panel of 357 kinases. Crystallographic  
25  
26 data collection and refinement statistics. Virtual screening led to the discovery of hit  
27  
28 compound. Dendrogram representation of the kinase selectivity profile of **25**.  
29  
30 Overview of X-ray co-crystal structure and a 2D ligand-interaction diagram of **25**.  
31  
32 Effects of **25** (20 nM and 100 nM) on the location and redistribution of SR proteins.  
33  
34 Detection of autophagy and autophagic flux induced by **25** (20 nM and 100 nM). *In*  
35  
36 *vitro* effects of **18** on LC3. Pharmacokinetic characteristics of **25**. IC<sub>50</sub> curves of **1**, **9e**,  
37  
38 and **25** on CLK1 and DYRK1A. IC<sub>50</sub> curves of **25** on remaining kinases whose  
39  
40 inhibitory rates were higher than 50% at 10 μM. Pharmacokinetic assessments of **25**.  
41  
42 Synthesis and structure confirmation of **25R** (the enantiomer of **25**). Copies of <sup>1</sup>H-  
43  
44 and <sup>13</sup>C-NMR spectra. Copies of MS spectra. HPLC purity analysis for **25**.  
45  
46 Confirmation of enantiomeric purity of **25**. Molecular formula strings (CSV).  
47  
48  
49  
50  
51  
52  
53  
54

### 55 Accession Codes

56  
57  
58  
59  
60

1  
2  
3  
4 Coordinates and structure factors for structures of **25** have been deposited in the  
5  
6 Protein Data Bank with the accession codes of 5X8I. Authors will release the atomic  
7  
8 coordinates and experimental data upon article publication.  
9  
10

## 11 12 13 14 **AUTHOR INFORMATION**

### 15 16 **Corresponding Author**

17  
18 \*Tel.: +86-28-85164063; Fax: +86-28-85164060; E-mail: luguangwen2001@126.com,  
19  
20 or yangsy@scu.edu.cn.  
21  
22

### 23 24 **ORCID**

25  
26 Guang-Wen Lu: 0000-0001-7568-592X  
27

28  
29 Sheng-Yong Yang: 0000-0001-5147-3746  
30

### 31 32 **Author Contributions**

33  
34 §Q.-Z. S., G.-F. L. and L.-L. L. contributed equally to this work.  
35

### 36 37 **Notes**

38  
39 The authors declare no competing financial interest.  
40  
41

### 42 43 44 **Acknowledgements**

45  
46 We thank Prof. Stefan Knapp for providing us the plasmid of CLK1. This work  
47  
48 was supported by the 973 Program (2013CB967204), the National Natural  
49  
50 Science Foundation of China (81325021, 81473140, 81573349, and 81522026),  
51  
52 and the Program for Changjiang Scholars and Innovative Research Team in  
53  
54  
55  
56  
57  
58  
59  
60

1  
2  
3  
4 University (IRT\_17R78). Prof. Guangwen Lu is in part supported by the State  
5  
6 Key Research Development Program of China (2016YFC1200300).  
7  
8  
9

## 10 11 **ABBREVIATIONS**

12  
13 CLK, cdc2-like kinase; DYRK, dual-specificity  
14  
15 tyrosine-phosphorylation-regulated kinase; SR proteins, serine/arginine-rich  
16  
17 proteins; LC3, microtubule-associated protein 1 light chain 3; mRFP,  
18  
19 mammalian red fluorescent protein; Ad-mRFP-GFP-LC3, adenovirus coding  
20  
21 tandem mRFP-GFP-LC3; DILI, drug-induced liver injury; H&E, hematoxylin  
22  
23 and eosin; APAP, Acetaminophen; ALT, alanine aminotransferase; AST,  
24  
25 aspartate aminotransferase.  
26  
27  
28  
29  
30  
31  
32

## 33 34 **REFERENCES**

- 35  
36 1. Janji, B.; Viry, E.; Moussay, E.; Paggetti, J.; Arakelian, T.; Mgrditchian, T.;  
37  
38 Messai, Y.; Noman, M. Z.; Van Moer, K.; Hasmmim, M.; Mami-Chouaib, F.; Berchem,  
39  
40 G.; Chouaib, S. The multifaceted role of autophagy in tumor evasion from immune  
41  
42 surveillance. *Oncotarget* **2016**, *7*, 17591-17607.  
43  
44  
45  
46 2. Lee, M. S. Role of islet beta cell autophagy in the pathogenesis of diabetes.  
47  
48 *Trends Endocrinol. Metab.* **2014**, *25*, 620-627.  
49  
50  
51 3. Riahi, Y.; Wikstrom, J. D.; Bachar-Wikstrom, E.; Polin, N.; Zucker, H.; Lee, M.  
52  
53 S.; Quan, W.; Haataja, L.; Liu, M.; Arvan, P.; Cerasi, E.; Leibowitz, G. Autophagy is  
54  
55 a major regulator of beta cell insulin homeostasis. *Diabetologia* **2016**, *59*, 1480-1491.  
56  
57  
58  
59  
60

- 1  
2  
3  
4 4. Frake, R. A.; Ricketts, T.; Menzies, F. M.; Rubinsztein, D. C. Autophagy and  
5  
6 neurodegeneration. *J. Clin. Invest.* **2015**, *125*, 65-74.  
7
- 8  
9 5. Menzies, F. M.; Fleming, A.; Rubinsztein, D. C. Compromised autophagy and  
10  
11 neurodegenerative diseases. *Nat. Rev. Neurosci.* **2015**, *16*, 345-357.  
12
- 13  
14 6. Ni, H. M.; Bockus, A.; Boggess, N.; Jaeschke, H.; Ding, W. X. Activation of  
15  
16 autophagy protects against acetaminophen-induced hepatotoxicity. *Hepatology* **2012**,  
17  
18 *55*, 222-232.  
19
- 20  
21 7. Ni, H. M.; Jaeschke, H.; Ding, W. X. Targeting autophagy for drug-induced  
22  
23 hepatotoxicity. *Autophagy* **2012**, *8*, 709-710.  
24
- 25  
26 8. Morel, E.; Mehrpour, M.; Botti, J.; Dupont, N.; Hamai, A.; Nascimbeni, A. C.;  
27  
28 Codogno, P. Autophagy: a druggable process. *Annu. Rev. Pharmacol. Toxicol.* **2017**,  
29  
30 *57*, 375-398.  
31
- 32  
33 9. Gros, F.; Muller, S. Pharmacological regulators of autophagy and their link with  
34  
35 modulators of lupus disease. *Br. J. Pharmacol.* **2014**, *171*, 4337-4359.  
36  
37
- 38  
39 10. Levine, B.; Packer, M.; Codogno, P. Development of autophagy inducers in  
40  
41 clinical medicine. *J. Clin. Invest.* **2015**, *125*, 14-24.  
42
- 43  
44 11. Breslin, E. M.; White, P. C.; Shore, A. M.; Clement, M.; Brennan, P. LY294002  
45  
46 and rapamycin co-operate to inhibit T-cell proliferation. *Br. J. Pharmacol.* **2005**, *144*,  
47  
48 791-800.  
49
- 50  
51 12. Coenen, J. J.; Koenen, H. J.; van Rijssen, E.; Hilbrands, L. B.; Joosten, I.  
52  
53 Rapamycin, and not cyclosporin A, preserves the highly suppressive CD27<sup>+</sup> subset of  
54  
55 human CD4<sup>+</sup>CD25<sup>+</sup> regulatory T cells. *Blood* **2006**, *107*, 1018-1023.  
56  
57  
58  
59  
60

- 1  
2  
3  
4 13. Houde, V. P.; Brule, S.; Festuccia, W. T.; Blanchard, P. G.; Bellmann, K.;  
5  
6 Deshaies, Y.; Marette, A. Chronic rapamycin treatment causes glucose intolerance  
7  
8 and hyperlipidemia by upregulating hepatic gluconeogenesis and impairing lipid  
9  
10 deposition in adipose tissue. *Diabetes* **2010**, *59*, 1338-1348.
- 11  
12  
13 14. Lamming, D. W.; Ye, L.; Katajisto, P.; Goncalves, M. D.; Saitoh, M.; Stevens, D.  
14  
15 M.; Davis, J. G.; Salmon, A. B.; Richardson, A.; Ahima, R. S.; Guertin, D. A.;  
16  
17 Sabatini, D. M.; Baur, J. A. Rapamycin-induced insulin resistance is mediated by  
18  
19 mTORC2 loss and uncoupled from longevity. *Science* **2012**, *335*, 1638-1643.
- 20  
21  
22 23. Fant, X.; Durieu, E.; Chicanne, G.; Payrastre, B.; Sbrissa, D.; Shisheva, A.;  
24  
25 Limanton, E.; Carreaux, F.; Bazureau, J. P.; Meijer, L. Cdc-like/dual-specificity  
26  
27 tyrosine phosphorylation-regulated kinases inhibitor leucettine L41 induces  
28  
29 mTOR-dependent autophagy: implication for Alzheimer's disease. *Mol. Pharmacol.*  
30  
31  
32 **2014**, *85*, 441-450.
- 33  
34  
35 36. Tahtouh, T.; Elkins, J. M.; Filippakopoulos, P.; Soundararajan, M.; Burgy, G.;  
36  
37 Durieu, E.; Cochet, C.; Schmid, R. S.; Lo, D. C.; Delhommel, F.; Oberholzer, A. E.;  
38  
39 Pearl, L. H.; Carreaux, F.; Bazureau, J.-P.; Knapp, S.; Meijer, L. Selectivity, cocrystal  
40  
41 structures, and neuroprotective properties of leucettines, a family of protein kinase  
42  
43 inhibitors derived from the marine sponge alkaloid leucettamine B. *J. Med. Chem.*  
44  
45  
46 **2012**, *55*, 9312-9330.
- 47  
48  
49 50. Debdab, M.; Carreaux, F.; Renault, S.; Soundararajan, M.; Fedorov, O.;  
51  
52 Filippakopoulos, P.; Lozach, O.; Babault, L.; Tahtouh, T.; Baratte, B.; Ogawa, Y.;  
53  
54 Hagiwara, M.; Eisenreich, A.; Rauch, U.; Knapp, S.; Meijer, L.; Bazureau, J.-P.  
55  
56  
57  
58  
59  
60

1  
2  
3  
4 Leucettines, a class of potent inhibitors of cdc2-like kinases and dual specificity,  
5  
6 tyrosine phosphorylation regulated kinases derived from the marine sponge  
7  
8 leucettamine B: modulation of alternative pre-RNA splicing. *J. Med. Chem.* **2011**, *54*,  
9  
10 4172-4186.

11  
12  
13 18. Giraud, F.; Alves, G.; Debiton, E.; Nauton, L.; Thery, V.; Durieu, E.; Ferandin,  
14  
15 Y.; Lozach, O.; Meijer, L.; Anizon, F.; Pereira, E.; Moreau, P. Synthesis, protein  
16  
17 kinase inhibitory potencies, and in vitro antiproliferative activities of meridianin  
18  
19 derivatives. *J. Med. Chem.* **2011**, *54*, 4474-4489.

20  
21  
22 19. Fedorov, O.; Huber, K.; Eisenreich, A.; Filippakopoulos, P.; King, O.; Bullock,  
23  
24 A. N.; Szklarczyk, D.; Jensen, L. J.; Fabbro, D.; Trappe, J.; Rauch, U.; Bracher, F.;  
25  
26 Knapp, S. Specific CLK inhibitors from a novel chemotype for regulation of  
27  
28 alternative splicing. *Chem. Biol.* **2011**, *18*, 67-76.

29  
30  
31 20. Esvan, Y. J.; Zeinyeh, W.; Boibessot, T.; Nauton, L.; Théry, V.; Knapp, S.;  
32  
33 Chaikuad, A.; Loaëc, N.; Meijer, L.; Anizon, F.; Giraud, F.; Moreau, P. Discovery of  
34  
35 pyrido[3,4-g]quinazoline derivatives as CMGC family protein kinase inhibitors:  
36  
37 design, synthesis, inhibitory potency and X-ray co-crystal structure. *Eur. J. Med.*  
38  
39 *Chem.* **2016**, *118*, 170-177.

40  
41  
42 21. Coombs, T. C.; Tanega, C.; Shen, M.; Wang, J. L.; Auld, D. S.; Gerritz, S. W.;  
43  
44 Schoenen, F. J.; Thomas, C. J.; Aubé, J. Small-molecule pyrimidine inhibitors of the  
45  
46 cdc2-like (CLK) and dual specificity tyrosine phosphorylation-regulated (DYRK)  
47  
48 kinases: development of chemical probe ML315. *Bioorg. Med. Chem. Lett.* **2013**, *23*,  
49  
50 3654-3661.  
51  
52  
53  
54  
55  
56  
57  
58  
59  
60

- 1  
2  
3  
4 22. Drung, B.; Scholz, C.; Barbosa, V. A.; Nazari, A.; Sarragiotto, M. H.; Schmidt,  
5  
6 B. Computational & experimental evaluation of the structure/activity  
7  
8 relationship of  $\beta$ -carbolines as DYRK1A inhibitors. *Bioorg. Med. Chem. Lett.* **2014**,  
9  
10 24, 4854-4860.  
11  
12  
13 23. Rachdi, L.; Kariyawasam, D.; Guez, F.; Aiello, V.; Arbones, M. L.; Janel, N.;  
14  
15 Delabar, J. M.; Polak, M.; Scharfmann, R. DYRK1A haploinsufficiency induces  
16  
17 diabetes in mice through decreased pancreatic beta cell mass. *Diabetologia* **2014**, *57*,  
18  
19 960-969.  
20  
21  
22 24. Fernandez-Martinez, P.; Zahonero, C.; Sanchez-Gomez, P. DYRK1A: the  
23  
24 double-edged kinase as a protagonist in cell growth and tumorigenesis. *Mol. Cell.*  
25  
26 *Oncol.* **2015**, *2*, e970048.  
27  
28  
29 25. Muraki, M.; Ohkawara, B.; Hosoya, T.; Onogi, H.; Koizumi, J.; Koizumi, T.;  
30  
31 Sumi, K.; Yomoda, J.; Murray, M. V.; Kimura, H.; Furuichi, K.; Shibuya, H.;  
32  
33 Krainer, A. R.; Suzuki, M.; Hagiwara, M. Manipulation of alternative splicing by a  
34  
35 newly developed inhibitor of CLKs. *J. Biol. Chem.* **2004**, *279*, 24246-24254.  
36  
37  
38 26. Degorce, S. L.; Barlaam, B.; Cadogan, E.; Dishington, A.; Ducray, R.; Glossop,  
39  
40 S. C.; Hassall, L. A.; Lach, F.; Lau, A.; McGuire, T. M.; Nowak, T.; Ouvry, G.; Pike,  
41  
42 K. G.; Thomason, A. G. Discovery of novel 3-quinoline carboxamides as potent,  
43  
44 selective, and orally bioavailable inhibitors of ataxia telangiectasia mutated (ATM)  
45  
46 kinase. *J. Med. Chem.* **2016**, *59*, 6281-6292.  
47  
48  
49 27. Glatthar, R.; Stojanovic, A.; Troxler, T.; Mattes, H.; Mobitz, H.; Beerli, R.;  
50  
51 Blanz, J.; Gassmann, E.; Druckes, P.; Fendrich, G.; Gutmann, S.; Martiny-Baron, G.;  
52  
53  
54  
55  
56  
57  
58  
59  
60

1  
2  
3  
4 Spence, F.; Hornfeld, J.; Peel, J. E.; Sparrer, H. Discovery of imidazoquinolines as a  
5  
6 novel class of potent, selective, and in vivo efficacious cancer osaka thyroid (COT)  
7  
8 kinase inhibitors. *J. Med. Chem.* **2016**, *59*, 7544-7560.

9  
10  
11 28. Haile, P. A.; Votta, B. J.; Marquis, R. W.; Bury, M. J.; Mehlmann, J. F.;  
12  
13 Singhaus, R., Jr.; Charnley, A. K.; Lakdawala, A. S.; Convery, M. A.; Lipshutz, D.  
14  
15 B.; Desai, B. M.; Swift, B.; Capriotti, C. A.; Berger, S. B.; Mahajan, M. K.; Reilly, M.  
16  
17 A.; Rivera, E. J.; Sun, H. H.; Nagilla, R.; Beal, A. M.; Finger, J. N.; Cook, M. N.;  
18  
19 King, B. W.; Ouellette, M. T.; Totoritis, R. D.; Pierdomenico, M.; Negroni, A.;  
20  
21 Stronati, L.; Cucchiara, S.; Ziolkowski, B.; Vossenkamper, A.; MacDonald, T. T.;  
22  
23 Gough, P. J.; Bertin, J.; Casillas, L. N. The identification and pharmacological  
24  
25 characterization of  
26  
27 6-(tert-butylsulfonyl)-*N*-(5-fluoro-1H-indazol-3-yl)quinolin-4-amine (GSK583), a  
28  
29 highly potent and selective inhibitor of RIP2 kinase. *J. Med. Chem.* **2016**, *59*,  
30  
31 4867-4880.  
32  
33

34  
35  
36  
37  
38 29. Jain, P.; Karthikeyan, C.; Moorthy, N. S.; Waiker, D. K.; Jain, A. K.; Trivedi, P.  
39  
40 Human cdc2-like kinase 1 (CLK1): a novel target for Alzheimer's disease. *Curr. Drug*  
41  
42 *Targets* **2014**, *15*, 539-550.  
43  
44

45  
46 30. Colwill, K.; Pawson, T.; Andrews, B.; Prasad, J.; Manley, J. L.; Bell, J. C.;  
47  
48 Duncan, P. I. The CLK/STY protein kinase phosphorylates SR splicing factors and  
49  
50 regulates their intranuclear distribution. *Embo J.* **1996**, *15*, 265-275.  
51  
52

53  
54 31. Xie, Z.; Nair, U.; Klionsky, D. J. Atg8 controls phagophore expansion during  
55  
56 autophagosome formation. *Mol. Biol. Cell* **2008**, *19*, 3290-3298.  
57  
58  
59  
60

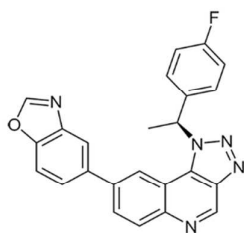


- 1  
2  
3  
4 32. Nakatogawa, H.; Ichimura, Y.; Ohsumi, Y. Atg8, a ubiquitin-like protein required  
5  
6 for autophagosome formation, mediates membrane tethering and hemifusion. *Cell*  
7  
8 **2007**, *130*, 165-178.
- 9  
10  
11 33. Kadowaki, M.; Karim, M. R. Cytosolic LC3 ratio as a quantitative index of  
12  
13 macroautophagy. *Methods Enzymol.* **2009**, *452*, 199-213.
- 14  
15  
16 34. Karim, M. R.; Kanazawa, T.; Daigaku, Y.; Fujimura, S.; Miotto, G.; Kadowaki,  
17  
18 M. Cytosolic LC3 ratio as a sensitive index of macroautophagy in isolated rat  
19  
20 hepatocytes and H4-II-E cells. *Autophagy* **2007**, *3*, 553-560.
- 21  
22  
23 35. Mizushima, N.; Yoshimori, T.; Levine, B. Methods in mammalian autophagy  
24  
25 research. *Cell* **2010**, *140*, 313-326.
- 26  
27  
28  
29 36. Singh, K.; Sharma, A.; Mir, M. C.; Drazba, J. A.; Heston, W. D.; Magi-Galluzzi,  
30  
31 C.; Hansel, D.; Rubin, B. P.; Klein, E. A.; Almasan, A. Autophagic flux determines  
32  
33 cell death and survival in response to Apo2L/TRAIL (dulanermin). *Mol. Cancer*  
34  
35 **2014**, *13*, 70.
- 36  
37  
38  
39 37. Chen, M.; Borlak, J.; Tong, W. A model to predict severity of drug-induced liver  
40  
41 injury in humans. *Hepatology* **2016**, *64*, 931-940.
- 42  
43  
44 38. Larson, A. M.; Polson, J.; Fontana, R. J.; Davern, T. J.; Lalani, E.; Hynan, L. S.;  
45  
46 Reisch, J. S.; Schiodt, F. V.; Ostapowicz, G.; Shakil, A. O.; Lee, W. M.  
47  
48 Acetaminophen-induced acute liver failure: results of a United States multicenter,  
49  
50 prospective study. *Hepatology* **2005**, *42*, 1364-1372.
- 51  
52  
53  
54  
55  
56  
57  
58  
59  
60

- 1  
2  
3  
4 39. Ni, H. M.; Williams, J. A.; Jaeschke, H.; Ding, W. X. Zonated induction of  
5  
6 autophagy and mitochondrial spheroids limits acetaminophen-induced necrosis in the  
7  
8 liver. *Redox Biol.* **2013**, *1*, 427-432.  
9  
10  
11 40. Kheloufi, M.; Boulanger, C. M.; Durand, F.; Rautou, P. E. Liver autophagy in  
12  
13 anorexia nervosa and acute liver injury. *BioMed Res. Int.* **2014**, *2014*, 701064.  
14  
15  
16 41. Wang, Q. S.; Yu, F.; Huang, S.; Sun, B.; Zhang, K. H.; Liu, K.; Wang, Z. J.; Xu,  
17  
18 C. Y.; Wang, S. S.; Yang, L. F.; Pan, Q. Y.; Li, L.; Zhou, H.; Cui, Y.; Xu, Q.;  
19  
20 Thomas, E.; He, J. H. The macromolecular crystallography beamline of SSRF. *Nucl.*  
21  
22 *Sci. Tech.* **2015**, *26*, 1-6.  
23  
24  
25  
26 42. Otwinowski, Z.; Minor, W. Processing of X-ray diffraction data collected in  
27  
28 oscillation mode. *Methods Enzymol.* **1997**, *276*, 307-326.  
29  
30  
31 43. Read, R. J. Pushing the boundaries of molecular replacement with maximum  
32  
33 likelihood. *Acta Crystallogr., Sect. D: Biol. Crystallogr.* **2001**, *57*, 1373-1382.  
34  
35  
36 44. Collaborative, C. P. The CCP4 suite: programs for protein crystallography. *Acta*  
37  
38 *Crystallogr., Sect. D: Biol. Crystallogr.* **1994**, *50*, 760-763.  
39  
40  
41 45. Murshudov, G. N.; Vagin, A. A.; Dodson, E. J. Refinement of macromolecular  
42  
43 structures by the maximum-likelihood method. *Acta Crystallogr., Sect. D: Biol.*  
44  
45 *Crystallogr.* **1997**, *53*, 240-255.  
46  
47  
48 46. Adams, P. D.; Afonine, P. V.; Bunkóczi, G.; Chen, V. B.; Davis, I. W.; Echols,  
49  
50 N.; Headd, J. J.; Hung, L.-W.; Kapral, G. J.; Grosse-Kunstleve, R. W. PHENIX: a  
51  
52 comprehensive Python-based system for macromolecular structure solution. *Acta*  
53  
54 *Crystallogr., Sect. D: Biol. Crystallogr.* **2010**, *66*, 213-221.  
55  
56  
57  
58  
59  
60

- 1  
2  
3  
4 47. Emsley, P.; Cowtan, K. Coot: model-building tools for molecular graphics. *Acta*  
5  
6 *Crystallogr., Sect. D: Biol. Crystallogr.* **2004**, *60*, 2126-2132.  
7  
8  
9  
10  
11  
12  
13  
14  
15  
16  
17  
18  
19  
20  
21  
22  
23  
24  
25  
26  
27  
28  
29  
30  
31  
32  
33  
34  
35  
36  
37  
38  
39  
40  
41  
42  
43  
44  
45  
46  
47  
48  
49  
50  
51  
52  
53  
54  
55  
56  
57  
58  
59  
60

## Table of Contents Graphic

**25** $IC_{50}(\text{CLK1}) = 2 \text{ nM}$  $IC_{50}(\text{DYRK1A}) = 138 \text{ nM}$ 